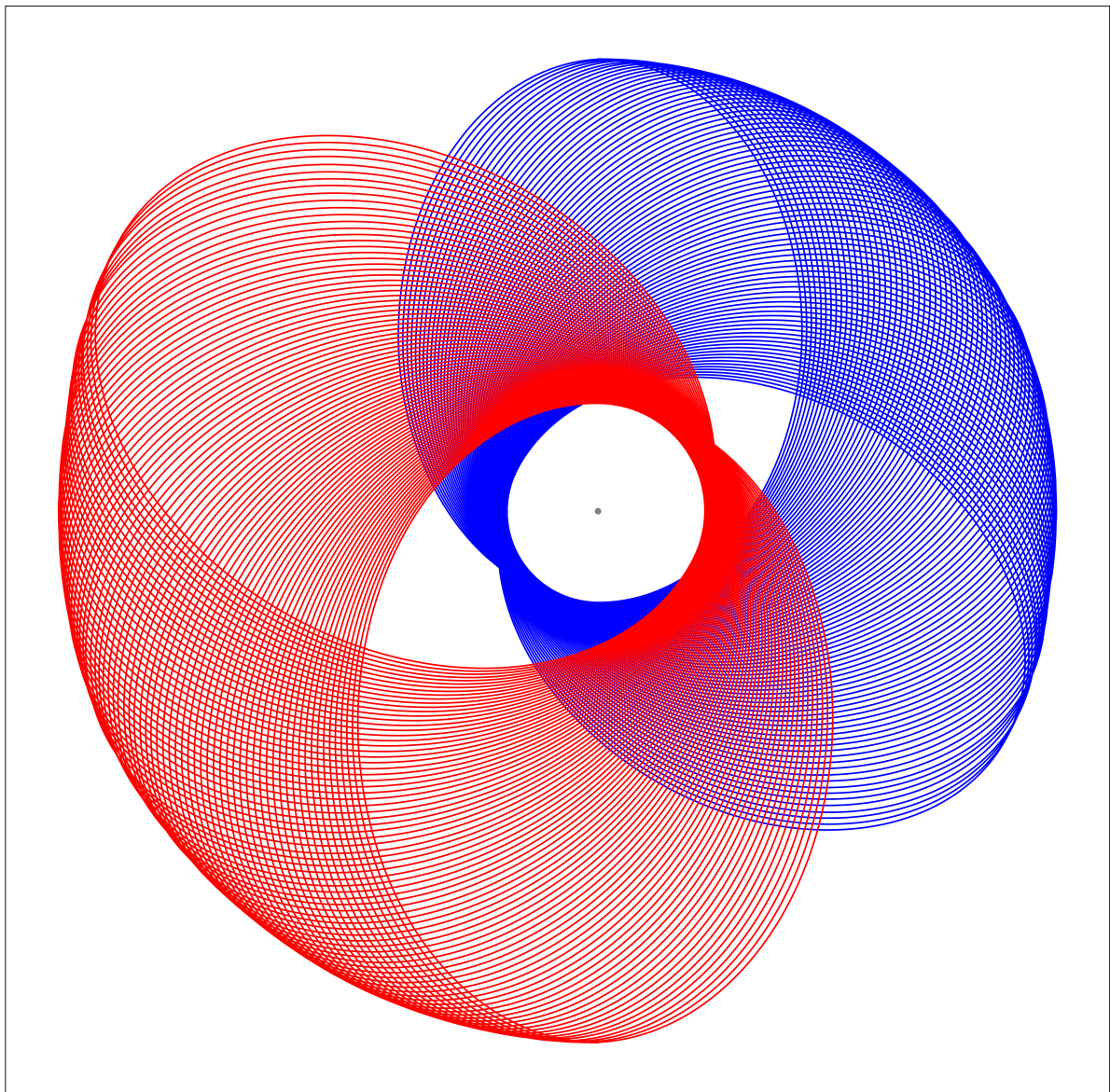


SCATTERING AND BOUND STATE ORBITS IN POST-MINKOWSKIAN GRAVITY

Numerically Simulating Orbits in General Relativity with Post-Newtonian and
Post-Minkowskian Corrections

Carl Ivarsen Askehave & Rögnvaldur Konráð Helgason



Abstract

The post-Minkowskian expansion is a way of correcting Newtonian equations of motion and potentials with respect to effects emerging from Einstein's theory of general relativity. In this paper, scattering and bound state orbits of two massive bodies will be numerically simulated in first and second post-Minkowskian expansions and compared with a first order post-Newtonian expansion as well as with classical Newtonian orbits. Furthermore, the paper will explore advantages of the post-Minkowskian expansion and develop a stronger intuition for the behaviour of post-Minkowskian equations of motion. The results of this research are that the performance of the post-Minkowskian expansion surpasses that of the post-Newtonian in ultra-relativistic regimes. This research could be expanded upon at higher orders of the expansions to further develop the simulation gravitational waveforms resulting from binary systems, which are instrumental for theoretical as well as experimental gravitational wave research.

NAME OF INSTITUTE: Niels Bohr Institute

AUTHORS: Carl Ivarsen Askehave & Rögnvaldur Konráð Helgason

EMAIL: wfq585@alumni.ku.dk & bnv384@alumni.ku.dk

TITLE AND SUBTITLE: Scattering and Bound State Orbits in Post-Minkowskian Gravity:
Numerically Simulating Orbits in General Relativity with Post-Newtonian and Post-Minkowskian Corrections

SUPERVISORS: Poul Henrik Damgaard & Johan Samsing

HANDED IN: 15.06.2022

DEFENDED: 27.06.2022

NAME: *Carl Ivarsen Askehave and Rögnvaldur Konráð Helgason*

SIGNATURE:  

DATE: *15/06/22*

Contents

1	Introduction	1
2	The Two-Body Problem in Classical Mechanics	1
2.1	The center of mass transformation	1
2.2	Two-body motion is planar	2
2.3	Hamiltonian mechanics	3
3	General Relativity	3
3.1	From Newton to Einstein	3
3.1.1	Minkowski space	3
3.1.2	The spacetime metric	4
3.1.3	Geodesics	4
3.1.4	The Einstein field equations	5
3.1.5	Corrections in general relativity	5
3.2	Post-Newtonian expansion	5
3.2.1	First-order post-Newtonian expansion	6
3.3	Post-Minkowskian expansion	7
3.3.1	First order post-Minkowskian expansion	7
3.3.2	Second order post-Minkowskian expansion	8
3.4	Relation between the PN and PM expansion	8
3.4.1	Recovering PN from PM expansions	8
3.4.2	The virial theorem	8
3.5	Analytical expressions for observables	9
3.5.1	Scattering angle	9
3.5.2	Periastron precession	10
3.5.3	Eccentricity	10
4	Numerical Methods	10
4.1	Units	11
4.2	Numerically solving the two-body problem	11
4.3	Extracting parameters from simulations	13
4.3.1	Scattering angle	13
4.3.2	Periastron precession	13
5	Results	14
5.1	Scattering systems	14
5.1.1	Ultra-relativistic scattering	14
5.1.2	Non-relativistic scattering	15
5.1.3	Scattering angle vs angular momentum	15
5.2	Bound systems	17
5.2.1	Non-eccentric similar mass binary system	17
5.2.2	Precession in eccentric test-body limit	18
5.2.3	Precession in eccentric similar mass binary system	19
5.2.4	Precession angle vs angular momentum	19
5.2.5	Relativistic Newtonian orbits	20
5.3	Conservation of energy and angular momentum	21
6	Conclusions and Further Work	22
Bibliography		25
A Post-Minkowskian Equations of Motion		i

1 Introduction

Gravitational waves (GWs) were predicted quite early by Albert Einstein in 1916 as presented in [10]. There he used a first order perturbative method in the weak field limit of gravity on the field equations of general relativity (GR) to linearize the equations and derive wave solutions describing fluctuations in the fabric of reality; spacetime. The existence of GWs was then confirmed almost 100 years later in 2015 by LIGO's observations of a binary black hole merger, made possible by modeling of such binary systems and their alleged gravitational waveforms. Due to the remarkably small amplitudes of GWs, modeling of this kind is essential, since it makes distinguishing the signal from background noise possible [1].

In order to describe binary neutron star and black hole systems accurately, it is necessary to make analytical approximations in GR. The most popular approximation has, by far, been the post-Newtonian (PN) expansion which is an expansion in the velocity, v/c , around zero. Despite the PN expansion being only formally valid in a low-velocity regime (compared to the speed of light) and weak gravity, it has had surprising success outside of those regimes [18], even being a successful tool in the discovery of gravitational waves by the LIGO and Virgo detectors. This use of the PN expansion is not without its limits though and that is where the post-Minkowskian (PM) expansion comes into play [5]. The PM expansion includes all orders of velocity but is expanded in Gm/rc^2 around zero, thus formally valid in weak gravity, but for any velocity, and can thus be used to analyse ultra-relativistic scattering and other cases that fall outside of the scope of the PN expansion.

Much has been written about the derivation of the various PM Hamiltonians but actual derivations of the equations of motion (EOM) (mainly the acceleration of the bodies in the system) from said Hamiltonians, and simulations, appear to be scarce within the literature. In this paper the Hamiltonian EOM for the 1PM and 2PM Hamiltonians, taken from [7], will be derived and simulated. Moreover the EOM of the 1PN expansion and a classical Newtonian system will be simulated for comparison. Important parameters affected by GR, such as the periastron precession and scattering angle, will be analyzed in particular by comparing simulations with analytical expressions. This analysis will result in a better understanding and intuition for the actual differences between the post-Newtonian and -Minkowskian expansions.

2 The Two-Body Problem in Classical Mechanics

The two-body problem (TBP) is an isolated system of two interacting massive bodies. This section will focus on solving the TBP, using classical and Hamiltonian mechanics, as well as showing how the test-body limit of the TBP reduces nicely to the one-body problem, i.e. movement of a single body in an external static gravitational field.

2.1 The center of mass transformation

Given two bodies, with masses m_1 and m_2 , positions \mathbf{r}_1 and \mathbf{r}_2 and velocities $\dot{\mathbf{r}}_1$ and $\dot{\mathbf{r}}_2$ respectively, one can find the position, \mathbf{R}_{CM} , and velocity, $\dot{\mathbf{R}}_{\text{CM}}$, of the center of mass in the inertial frame, using the conservation of momentum. The velocity $\dot{\mathbf{R}}_{\text{CM}}$ will in general be constant due to the system being isolated, i.e. no external force is acting upon it:

$$\mathbf{R}_{\text{CM}} = \frac{m_1 \mathbf{r}_1 + m_2 \mathbf{r}_2}{M}, \quad \dot{\mathbf{R}}_{\text{CM}} = \frac{m_1 \dot{\mathbf{r}}_1 + m_2 \dot{\mathbf{r}}_2}{M} = \text{const} \quad \text{and} \quad \ddot{\mathbf{R}}_{\text{CM}} = \frac{m_1 \ddot{\mathbf{r}}_1 + m_2 \ddot{\mathbf{r}}_2}{M} = \mathbf{0}, \quad (1)$$

where $M = m_1 + m_2$. Using the relative distance, $\mathbf{r} = \mathbf{r}_1 - \mathbf{r}_2$, one can rewrite:

$$\mathbf{r}_1 = \mathbf{R}_{\text{CM}} + \frac{m_2}{M} \mathbf{r}, \quad \mathbf{r}_2 = \mathbf{R}_{\text{CM}} - \frac{m_1}{M} \mathbf{r}. \quad (2)$$

Now, using Newton's second and third law, one has $\mathbf{F}_{21} = m_1 \ddot{\mathbf{r}}_1 = -m_2 \ddot{\mathbf{r}}_2 = -\mathbf{F}_{12}$,

$$m_2 \mathbf{F}_{21} - m_1 \mathbf{F}_{12} = m_1 m_2 (\ddot{\mathbf{r}}_1 - \ddot{\mathbf{r}}_2) \quad (3)$$

$$(m_2 + m_1) \mathbf{F}_{21} = m_1 m_2 \left(\frac{m_2}{m_1 + m_2} \ddot{\mathbf{r}} + \frac{m_1}{m_1 + m_2} \ddot{\mathbf{r}} \right) \quad (4)$$

$$\mathbf{F}_{21} = \frac{m_1 m_2}{m_1 + m_2} \left(\frac{m_1 + m_2}{m_1 + m_2} \ddot{\mathbf{r}} \right) = \frac{m_1 m_2}{m_1 + m_2} \ddot{\mathbf{r}}. \quad (5)$$

Knowing that for a central potential $\mathbf{F} = -\nabla V$, one arrives at

$$\mu \ddot{\mathbf{r}} = -\nabla V \quad (6)$$

where $\mu = m_1 m_2 / (m_1 + m_2)$ is the reduced mass [12].

Thus, the problem has been reduced from having to solve for the motion of both bodies $\mathbf{r}_1(t)$ and $\mathbf{r}_2(t)$ separately, to solving for the relative motion, $\mathbf{r}(t)$, in the center of mass frame, and then using equations (2) to find the positions of each individual body after solving.

Example: The one-body problem Looking at the TBP in the limit where $m_1 = m \ll M = m_2$, which is called the test-body limit of the TBP. Here, it is seen that

$$(1) \rightarrow \mathbf{R}_{CM} = \mathbf{r}_2, \quad \dot{\mathbf{R}}_{CM} = \dot{\mathbf{r}}_2, \quad \ddot{\mathbf{R}}_{CM} = \ddot{\mathbf{r}}_2 = \mathbf{0} \quad (7)$$

$$(2) \rightarrow \mathbf{r}_2 = \mathbf{r}_2, \quad \mathbf{r}_1 - \mathbf{r} = \mathbf{r}_2 \quad (8)$$

$$(6) \rightarrow m(\ddot{\mathbf{r}}_1 - \ddot{\mathbf{r}}_2) = m\ddot{\mathbf{r}}_1. \quad (9)$$

Thus, in this limit, the TBP completely reduces to the problem of one body with mass m subject to a conservative force due to an external potential $\mathbf{F} = -\nabla V$ centered at \mathbf{r}_2 . This is also called the one-body problem.

Using a classical Newtonian gravitational potential $V(r) = -Gm_1 m_2 / r$, where $G = 6.6743 \cdot 10^{-11} \text{ m}^3 \text{ kg}^{-1} \text{ s}^{-2}$ is Newton's gravitational constant, the gravitational force on the body with mass m then becomes

$$m\ddot{\mathbf{r}} = \mathbf{F} = -\nabla V(r) = -\frac{GMm}{r^2}\hat{\mathbf{r}}. \quad (10)$$

Given an initial position and velocity, this can then be integrated¹ to give the position of the body at any time t ,

$$\mathbf{r}(t) = \iint \ddot{\mathbf{r}}(t) dt^2 = -GM \iint \frac{\hat{\mathbf{r}}}{r(t)^2} dt^2. \quad (11)$$

Now the one-body problem has been solved for a traditional Newtonian gravitational potential, which has been shown to be equivalent to solving the TBP, although one needs to do the correct variable transformation.

2.2 Two-body motion is planar

When expanding the vector notation used above into each spatial component, one gets a system of equations which in Cartesian coordinates looks like

$$\mu \ddot{r}_x = -\frac{\partial V}{\partial x}, \quad \mu \ddot{r}_y = -\frac{\partial V}{\partial y} \quad \text{and} \quad \mu \ddot{r}_z = -\frac{\partial V}{\partial z}. \quad (12)$$

If \mathbf{r} is the relative position between two bodies and \mathbf{p} is their relative momentum, then the angular momentum \mathbf{L} is described as

$$\mathbf{L} = \mathbf{r} \times \mathbf{p} = \mathbf{r} \times \mu \dot{\mathbf{r}}. \quad (13)$$

It can be seen from the conservation of angular momentum

$$\frac{d\mathbf{L}}{dt} = \frac{d}{dt}(\mathbf{r} \times \mu \dot{\mathbf{r}}) = \mathbf{0}, \quad (14)$$

that the displacement vector \mathbf{r} and its rate of change $\dot{\mathbf{r}}$ will be in the plane perpendicular to the constant vector \mathbf{L} at all times t [17]. Thus, by a certain transformation of coordinates, more precisely the rotation that brings the \mathbf{r} and $\dot{\mathbf{r}}$ vectors into the x, y -plane, one can reduce the amount of equations from 3 to only 2:

$$\mu \ddot{r}_x = -\frac{\partial V}{\partial x}, \quad \mu \ddot{r}_y = -\frac{\partial V}{\partial y} \quad \text{and} \quad \mu \ddot{r}_z = -\frac{\partial V}{\partial z} = 0, \quad (15)$$

since the last one is trivial.

¹A derivation of the analytical solution of the orbit can be found in [11], but since the equations will be solved numerically, this is not of that big concern here.

2.3 Hamiltonian mechanics

Hamiltonian mechanics rest on entirely different principles than Newtonian mechanics, but have been shown to be equivalent (i.e. leading to the same EOM and hence the same physics) [15].

The power of Hamiltonian Mechanics comes from the fact that it is generally coordinate independent. If one wishes to describe a system of N bodies in motion in 3-dimensional space, then this has $n = 3N$ degrees of freedom, and can be described by the coordinates

$$x_i \quad \text{for } i = (1, 2, 3), (4, 5, 6), \dots, (n-2, n-1, n), \quad (16)$$

where the first triplet refers to the first body, the second triplet refers to the second body and so on [11]. Given k holonomic constraints of the system, then the Hamiltonian can in general be described by $2m = (n - k)$ generalized coordinates q_σ and momenta p_σ (for $\sigma = 1, \dots, m$) and maybe even time t :

$$H = H(q_1, \dots, q_m; p_1, \dots, p_m; t). \quad (17)$$

An example of such a constraint is given by the last expression in equation 15, that arises from the conservation of angular momentum.

Equation 17, coupled with the Hamiltonian EOM

$$\dot{q}_\sigma = \frac{\partial H}{\partial p_\sigma}, \quad \text{and} \quad \dot{p}_\sigma = -\frac{\partial H}{\partial q_\sigma} \quad (18)$$

gives $2m$ coupled first order differential equations in the time, which then determine the subsequent motion of the bodies [11]. Note that one can choose any generalized coordinates, as long as they describe the system and its constraints fully, and thus Hamiltonian mechanics is invariant to different coordinate changes, making it a powerful tool to solve a variety of different mechanical problems. This is related to gauge-invariance, since you can add a constant to the Hamiltonian and still get the same EOM, but that is outside the scope of this paper.

For a conservative system the Hamiltonian describes the total conserved energy

$$H = T + V = E = \text{const}, \quad (19)$$

where T and V are the kinetic and potential energies, and the Hamiltonian equations (18) then result in the same EOM as Newton's laws for the conserved system in question [11]. An example of how one solves a problem using Hamiltonian mechanics can be seen in Section 4.2.

3 General Relativity

In 1915 Albert Einstein published his theory of General Relativity (GR) which, in a sense, is an extension of Newtons theory of gravity to regimes where the force of gravity, or the relative velocity of bodies, is very large. One of the main points of GR is that gravity is a manifestation of the geometry of the 4-dimensional spacetime that makes up the universe.

3.1 From Newton to Einstein

3.1.1 Minkowski space

In Einsteins theory of Special Relativity, space and time are related and inseparable and this medium of the universe is described by the 4 coordinates

$$x^0 = c t, \quad x^1 = x, \quad x^2 = y, \quad x^3 = z, \quad (20)$$

where c is the speed of light [13]. Describing the 4 spacetime coordinates using the expression x^μ , $\mu = 0, 1, 2, 3$, and defining the infinitesimal distance between two events x^μ and $x^\mu + dx^\mu$ as dx^μ , then one can describe the infinitesimal *line-element* in flat spacetime as

$$ds^2 = \eta_{\mu\nu} dx^\mu dx^\nu = -(dx^0)^2 + (dx^1)^2 + (dx^2)^2 + (dx^3)^2, \quad (21)$$

where the *Einstein summation convention* is used to sum over the repeated indices μ and ν . Here the Minkowski metric

$$\eta_{\mu\nu} = \begin{pmatrix} -1 & 0 & 0 & 0 \\ 0 & 1 & 0 & 0 \\ 0 & 0 & 1 & 0 \\ 0 & 0 & 0 & 1 \end{pmatrix}, \quad (22)$$

is used to describe flat spacetime, also called *Minkowski space*. The theory of Special Relativity is the study of Minkowski space.

3.1.2 The spacetime metric

Since GR is a theory of geometry, and the metric is the object that manifests this geometry, it is of fundamental importance. In the evaluation of the line element ds^2 in flat spacetime, the Minkowski metric is used, although in general, one could have used any metric $g_{\mu\nu}$ describing any geometry of spacetime. The spacetime metric is a symmetric tensor $g_{\mu\nu} = g_{\nu\mu}$ which describes the curvature of spacetime, and it is often useful to write it as a 4×4 -matrix, as so

$$g_{\mu\nu} = \begin{pmatrix} g_{00} & g_{01} & g_{02} & g_{03} \\ g_{01} & g_{11} & g_{12} & g_{13} \\ g_{02} & g_{12} & g_{22} & g_{23} \\ g_{03} & g_{13} & g_{23} & g_{33} \end{pmatrix}. \quad (23)$$

The metric is what determines the geometry of, and thus, distances in the spacetime. Therefore the expressions for the line-element in a general spacetime is actually

$$ds^2 = g_{\mu\nu} dx^\mu dx^\nu. \quad (24)$$

3.1.3 Geodesics

In the flat Minkowski space of Special Relativity, a body not subject to external forces will follow a straight line through the flat spacetime. For more general spacetimes, this fact still applies, but now the curvature of the spacetime bends the straight lines, and the apparent trajectories aren't perceived as straight lines anymore. Such trajectories are called *geodesics*, and are described by the *geodesic equation*²

$$\frac{d^2x^\mu}{d\tau^2} + \Gamma_{\nu\rho}^\mu \frac{dx^\nu}{d\tau} \frac{dx^\rho}{d\tau} = 0, \quad (25)$$

where $u^\mu = dx^\mu/d\tau$ and $a^\mu = d^2x^\mu/d\tau^2$ are the relativistic velocity and acceleration respectively and the Christoffel Symbol $\Gamma_{\nu\rho}^\mu$ is a function of the metric, and embodies the curvature of the spacetime.

Newton limit of the geodesic equation Assuming (a) weak gravity, (b) static gravity and (c) small velocities is called the Newton limit, and these assumptions can be expressed mathematically as

$$(a) \quad g_{\mu\nu} = \eta_{\mu\nu} + h_{\mu\nu}, \quad (b) \quad \frac{\partial g_{\mu\nu}}{\partial t} = 0, \quad (c) \quad \left| \frac{dx^i}{dt} \right| \ll c \quad \text{for } i = 1, 2, 3. \quad (26)$$

where $|h_{\mu\nu}| \ll 1$. In this limit the geodesic equation reduces to³

$$\frac{d^2x^i}{dt^2} = \frac{1}{2} \frac{\partial h_{00}}{\partial x^i} \quad \text{for } i = 1, 2, 3, \quad (27)$$

and 0 in the case where $i = 0$. Comparing to Newtonian gravity

$$\frac{d^2x^i}{dt^2} = -\frac{1}{m} \frac{\partial V}{\partial x^i} \quad \text{for } i = 1, 2, 3, \quad (28)$$

²An excellent and concise derivation can be found in [13].

³Again, see [13] for the derivation.

it can be seen that

$$V = -\frac{m}{2} h_{00}. \quad (29)$$

This means that the small perturbation to the Minkowski metric is directly proportional to the Newtonian gravitational potential, V , confirming the fact that gravity is the same as the geometry of spacetime in the theory of GR. Using a perturbative approach, one can expand in $h_{\mu\nu}$ and achieve corrections to the gravitational potential to any wanted order of precision. This method is what leads to the theories of the post-Newtonian and the post-Minkowskian expansions.

3.1.4 The Einstein field equations

The Einstein field equations (EFE) are a set of non-linear partial differential equations that are the general relativistic generalization of Poissons equation $\nabla^2 V = 4\pi G \rho_m$, analogous to how the metric is the GR generalization of the gravitational potential V . Poissons equation relates gravitational potential to matter density. The EFE can be written as

$$R_{\mu\nu} - \frac{1}{2} g_{\mu\nu} R = \frac{8\pi G}{c^4} T_{\mu\nu}, \quad (30)$$

where $T_{\mu\nu}$ is the stress-energy tensor, $R_{\mu\nu}$ is the Ricci curvature tensor and R is its trace, called the Ricci scalar. The Ricci curvature tensor depends on $g_{\mu\nu}$ and embodies the curvature of a spacetime. Equations (30) then relate said curvature to the density and flux of energy and momentum in the spacetime [6].

Due to the non-linearity of the EFE it is cumbersome to find exact solutions, and in most cases even impossible. There do, however, exist exact solutions, such as ones obtained using the Schwarzschild and Kerr metrics, that have proven to be exceptionally useful for understanding black holes but which are limited in application due to their derivations assuming high levels of symmetry and simplicity, not representative of real world phenomena. For more practical applications of GR it is, therefore, useful and necessary to find approximate solutions using expansions in certain parameters.

3.1.5 Corrections in general relativity

The most common way to find approximate solutions to problems in general relativity is, as was shown in Section 3.1.3, to start with a flat Minkowskian spacetime and then add correction terms [18]. Then, since the metric is directly proportional to the gravitational potential, one can use this method to add small relativistic correction terms to a classical gravitational potential. Two such methods will be explored here.

3.2 Post-Newtonian expansion

The post-Newtonian (PN) expansion is an expansion in the parameter $v^2/c^2 \sim GM/rc^2$ (the validity of this proportionality is due to the virial theorem⁴), where v is the relative velocity, r is the relative distance and M is the total mass of the binary system [2]. This means that for an n th-order expansion one gets:

$$\sum_{i=0}^n \sum_{j=0}^i v^{2j} G^{(n+1)-i} \quad (31)$$

as can be seen in Table 1.

⁴See Section 3.4

	0PN	1PN	2PN	3PN	4PN	5PN	6PN	7PN										
1PM	(1	+	v^2	+	v^4	+	v^6	+	v^8	+	v^{10}	+	v^{12}	+	v^{14}	+	\dots)	G^1
2PM			(1	+	v^2	+	v^4	+	v^6	+	v^8	+	v^{10}	+	v^{12}	+	\dots)	G^2
3PM				(1	+	v^2	+	v^4	+	v^6	+	v^8	+	v^{10}	+	\dots)	G^3	
4PM					(1	+	v^2	+	v^4	+	v^6	+	v^8	+	\dots)	G^4		
5PM						(1	+	v^2	+	v^4	+	v^6	+	v^8	+	\dots)	G^5	
6PM							(1	+	v^2	+	v^4	+	v^6	+	\dots)	G^6		

Table 1: Comparison table of powers used for PN and PM approximations in the case of two non-rotating bodies. 0PN corresponds to the case of Newton's theory of gravitation. 0PM (not shown) corresponds to the Minkowski flat space. (Source: Wikipedia [16])

The PN expansion has been one of the most important methods for finding approximate solutions to problems in GR, the two-body problem (TBP) in particular. Since the expansion is made in the velocity and the gravitational parameter G , the PN expansion is only formally valid at low velocities, compared to the speed of light, as well as in a weak gravitational field [5].

3.2.1 First-order post-Newtonian expansion

Equations of motion for the TBP in first order post-Newtonian (1PN) expansion were first derived by Einstein, Infeld and Hoffmann (EIH) and are today found in various forms within the literature. The equation for the acceleration of one of the bodies in a binary system is given in [4] as:

$$\mathbf{a}_1 = -\frac{Gm_2}{r^3}\mathbf{r} + \frac{1}{c^2} \left\{ \left[\frac{5G^2m_1m_2}{r^3} + \frac{4G^2m_2^2}{r^3} + \frac{Gm_2}{r^2} \left(\frac{3}{2r}(\mathbf{r} \cdot \mathbf{v}_2)^2 - \mathbf{v}_1^2 + 4(\mathbf{v}_1 \cdot \mathbf{v}_2) - 2\mathbf{v}_2^2 \right) \right] \frac{\mathbf{r}}{r} + \frac{Gm_2}{r^3} \left[4(\mathbf{r} \cdot \mathbf{v}_1) - 3(\mathbf{r} \cdot \mathbf{v}_2) \right] \mathbf{v} \right\} \quad (32)$$

where \mathbf{r} and \mathbf{v} are the relative position and velocity vectors between the bodies, r and v are their lengths while \mathbf{v}_1 and \mathbf{v}_2 are the velocity vectors for each individual body.

The acceleration for body 2, \mathbf{a}_2 , is then found by exchanging 1 \longleftrightarrow 2 and letting $\mathbf{v}, \mathbf{r} \longleftrightarrow -\mathbf{v}, -\mathbf{r}$. These equations are then rewritten to a center of mass frame using equations (2):

$$\mathbf{a}_1 = -\frac{Gm_2}{r^3}\mathbf{r} + \frac{1}{c^2} \left\{ \left[\frac{5G^2m_1m_2}{r^3} + \frac{4G^2m_2^2}{r^3} + \frac{Gm_2}{r^2} \left(\frac{3}{2r} \frac{m_1^2}{M^2} (\mathbf{r} \cdot -\mathbf{v})^2 - \frac{m_2^2}{M^2} \mathbf{v}^2 + 4 \frac{m_2}{M} \frac{m_1}{M} (\mathbf{v} \cdot -\mathbf{v}) - 2 \frac{m_1^2}{M^2} (-\mathbf{v})^2 \right) \right] \frac{\mathbf{r}}{r} + \frac{Gm_2}{r^3} \left[4 \frac{m_2}{M} (\mathbf{r} \cdot \mathbf{v}) - 3 \frac{m_1}{M} (\mathbf{r} \cdot -\mathbf{v}) \right] \mathbf{v} \right\} \quad (33)$$

$$\mathbf{a}_2 = +\frac{Gm_2}{r^3}\mathbf{r} - \frac{1}{c^2} \left\{ \left[\frac{5G^2m_1m_2}{r^3} + \frac{4G^2m_1^2}{r^3} + \frac{Gm_1}{r^2} \left(\frac{3}{2r} \frac{m_2^2}{M^2} (-\mathbf{r} \cdot \mathbf{v})^2 - \frac{m_1^2}{M^2} (-\mathbf{v})^2 + 4 \frac{m_1}{M} \frac{m_2}{M} (-\mathbf{v} \cdot \mathbf{v}) - 2 \frac{m_2^2}{M^2} \mathbf{v}^2 \right) \right] \frac{\mathbf{r}}{r} + \frac{Gm_1}{r^3} \left[4 \frac{m_1}{M} (-\mathbf{r} \cdot -\mathbf{v}) - 3 \frac{m_2}{M} (-\mathbf{r} \cdot \mathbf{v}) \right] \mathbf{v} \right\}. \quad (34)$$

The relative acceleration is then obtained by $\mathbf{a} = \mathbf{a}_1 - \mathbf{a}_2$ and using $\mathbf{v} = \mathbf{p}/\mu = \mathbf{p} M/m_1 m_2$:

$$\mathbf{a} = -\frac{G(m_1 + m_2)}{r^3} \mathbf{r} + \frac{1}{c^2} \left\{ \left[\frac{10G^2 m_1 m_2}{r^3} + \frac{4G^2(m_1^2 + m_2^2)}{r^3} + \frac{G}{r^2} \left(\frac{3}{2r} \left(\frac{1}{m_1} + \frac{1}{m_2} \right) (\mathbf{r} \cdot \mathbf{p})^2 \right. \right. \right. \\ \left. \left. \left. - \frac{m_1^3 + m_2^3}{m_1^2 m_2^2} \mathbf{p}^2 - 6 \left(\frac{1}{m_1} + \frac{1}{m_2} \right) \mathbf{p}^2 \right) \right] \frac{\mathbf{r}}{r} + \frac{G}{r^3} \left[4 \frac{m_1^2 + m_2^2}{m_1 m_2} + 6 \right] \frac{(m_1 + m_2)(\mathbf{r} \cdot \mathbf{p})}{m_1 m_2} \mathbf{p} \right\}. \quad (35)$$

3.3 Post-Minkowskian expansion

Another method of finding approximate solutions in GR is the post-Minkowskian (PM) expansion. It is inherently a perturbation theory where one expands in the parameter Gm/rc^2 and includes all orders of v , unlike for the PN expansion. The PM expansion can be found by approaching the problem from an effective field theory of quantum gravity using relativistic scattering amplitudes [14], due to scattering amplitudes appearing as power series expansions in orders of G [2]. The PM expansion is thus valid in a highly relativistic regime and weak gravity, and is therefore very useful in modeling ultra-relativistic scattering [5].

3.3.1 First order post-Minkowskian expansion

Given the first order post-Minkowskian Hamiltonian in a COM frame from [7],

$$H_{1\text{PM}}(p, r) = E_1 + E_2 + V_{1\text{PM}}(p, r) = E_1 + E_2 + \frac{1}{E_1 E_2} \frac{G c_1}{r}, \quad (36)$$

where

$$c_1 = m_1^2 m_2^2 c^4 - 2 \left(\frac{E_1 E_2}{c^2} + p^2 \right)^2, \quad E_i = \sqrt{m_i^2 c^4 + p^2 c^2} \quad (37)$$

The Hamiltonian EOM are:

$$\dot{\mathbf{r}} = \frac{\partial H_{1\text{PM}}}{\partial \mathbf{p}} = \frac{\partial E_1}{\partial \mathbf{p}} + \frac{\partial E_2}{\partial \mathbf{p}} + \frac{G}{E_1^2 E_2^2 r} \left[E_1 E_2 \frac{\partial c_1}{\partial \mathbf{p}} - c_1 \left(\frac{\partial E_1}{\partial \mathbf{p}} E_2 + E_1 \frac{\partial E_2}{\partial \mathbf{p}} \right) \right] \quad (38)$$

$$\dot{\mathbf{p}} = -\frac{\partial H_{1\text{PM}}}{\partial \mathbf{r}} = \frac{G c_1}{E_1 E_2 r^3} \mathbf{r}, \quad (39)$$

where the equations are, again, formulated in a center of mass frame as described for the 1PN EOM in Section 3.2.1.

The acceleration can then be obtained:

$$\ddot{\mathbf{r}} = \frac{d}{dt} \frac{\partial E_1}{\partial \mathbf{p}} + \frac{d}{dt} \frac{\partial E_2}{\partial \mathbf{p}} \quad (40)$$

$$+ \frac{G}{E_1^2 E_2^2 r} \left\{ - \left(\dot{r} + 2 \frac{\dot{E}_1}{E_1} + 2 \frac{\dot{E}_2}{E_2} \right) \left[E_1 E_2 \frac{\partial c_1}{\partial \mathbf{p}} - c_1 \left(\frac{\partial E_1}{\partial \mathbf{p}} E_2 + E_1 \frac{\partial E_2}{\partial \mathbf{p}} \right) \right] \right. \\ \left. + \left[\left(\dot{E}_1 E_2 + E_1 \dot{E}_2 \right) \frac{\partial c_1}{\partial \mathbf{p}} + E_1 E_2 \frac{d}{dt} \frac{\partial c_1}{\partial \mathbf{p}} - \dot{c}_1 \left(\frac{\partial E_1}{\partial \mathbf{p}} E_2 + E_1 \frac{\partial E_2}{\partial \mathbf{p}} \right) \right. \right. \\ \left. \left. - c_1 \left(\frac{d}{dt} \frac{\partial E_1}{\partial \mathbf{p}} E_2 + \frac{\partial E_1}{\partial \mathbf{p}} \dot{E}_2 + E_1 \frac{\partial E_2}{\partial \mathbf{p}} + E_1 \frac{d}{dt} \frac{\partial E_2}{\partial \mathbf{p}} \right) \right] \right\} \quad (41)$$

where

$$\dot{c}_1 = -4 \left(\frac{E_1 E_2}{c^2} + p^2 \right) \left[\frac{1}{c^2} \left(\dot{E}_1 E_2 + E_1 \dot{E}_2 \right) + 2\mathbf{p} \cdot \dot{\mathbf{p}} \right] \quad (42)$$

$$\frac{\partial c_1}{\partial \mathbf{p}} = -4 \left(\frac{E_1 E_2}{c^2} + p^2 \right) \left[\frac{1}{c^2} \left(\frac{\partial E_1}{\partial \mathbf{p}} E_2 + E_1 \frac{\partial E_2}{\partial \mathbf{p}} \right) + 2\mathbf{p} \right] \quad (43)$$

$$\begin{aligned} \frac{d}{dt} \frac{\partial c_1}{\partial \mathbf{p}} = & -4 \left(\left[\frac{1}{c^2} \left(\dot{E}_1 E_2 + E_1 \dot{E}_2 \right) + 2\mathbf{p} \cdot \dot{\mathbf{p}} \right] \left[\frac{1}{c^2} \left(\frac{\partial E_1}{\partial \mathbf{p}} E_2 + E_1 \frac{\partial E_2}{\partial \mathbf{p}} \right) + 2\mathbf{p} \right] \right. \\ & \left. + \left(\frac{E_1 E_2}{c^2} + p^2 \right) \left[\frac{1}{c^2} \left(\frac{d}{dt} \frac{\partial E_1}{\partial \mathbf{p}} E_2 + \frac{\partial E_1}{\partial \mathbf{p}} \dot{E}_2 + \dot{E}_1 \frac{\partial E_2}{\partial \mathbf{p}} + E_1 \frac{d}{dt} \frac{\partial E_2}{\partial \mathbf{p}} \right) + 2\dot{\mathbf{p}} \right] \right) \end{aligned} \quad (44)$$

along with

$$\frac{\partial E_i}{\partial \mathbf{p}} = \frac{c^2}{E_i} \mathbf{p}, \quad \dot{E}_i = \frac{\partial E_i}{\partial \mathbf{p}} \cdot \dot{\mathbf{p}} \quad \text{and} \quad \frac{d}{dt} \frac{\partial E_i}{\partial \mathbf{p}} = \frac{c^2}{E_i} \dot{\mathbf{p}} - \frac{c^2}{E_i^2} \dot{E}_i \mathbf{p}. \quad (45)$$

These equations will not be expanded in terms of \mathbf{r} and \mathbf{p} in order to save space.

3.3.2 Second order post-Minkowskian expansion

Now adding the second order PM correction term, the post-Minkowskian Hamiltonian from [7] becomes:

$$H_{2\text{PM}}(p, r) = E_1 + E_2 + V_{1\text{PM}}(p, r) + V_{2\text{PM}}(p, r) \quad (46)$$

where

$$\begin{aligned} V_{2\text{PM}}(p, r) = & \frac{G^2}{E_1 E_2 r^2} \left[\frac{1}{4c^2} \left(\frac{c_\triangleright}{m_1} + \frac{c_\triangleleft}{m_2} \right) \right. \\ & \left. + \frac{c_1(E_1 + E_2)}{E_1 E_2} \left(\frac{c_1}{2} \left(\frac{1}{(E_1 + E_2)^2} - \frac{1}{E_1 E_2} \right) - \frac{4}{c^2} \left(\frac{E_1 E_2}{c^2} + p^2 \right) \right) \right], \end{aligned} \quad (47)$$

with c_1 defined above in equation (37) and the other coefficients given by

$$c_\triangleright = 3m_1^2 \left(m_1^2 m_2^2 c^4 - 5 \left(\frac{E_1 E_2}{c^2} + p^2 \right)^2 \right) \quad \text{and} \quad c_\triangleleft = 3m_2^2 \left(m_1^2 m_2^2 c^4 - 5 \left(\frac{E_1 E_2}{c^2} + p^2 \right)^2 \right) \quad (48 \text{ a,b})$$

The subsequent derivation of the EOM has been moved to Appendix A due to its size.

3.4 Relation between the PN and PM expansion

3.4.1 Recovering PN from PM expansions

Due to the PM expansion including all orders of v for each order of G , as previously mentioned, it is possible to recover the PN from the PM expansions. This is considered to be another one of the strengths of the PM expansion. Looking at the diagonal in table 1, one can see that, for example, Taylor expanding the 1PM expansion to first order in the velocity term, v^2 , the 2PM to zeroth order in v^2 and adding them together, one recovers the 1PN expansion.

3.4.2 The virial theorem

The virial theorem is a relationship between the time averages of the kinetic energy, $\langle T \rangle$, and potential energy, $\langle V \rangle$, within a system. It states that the two can be thought of as proportional:

$$\langle T \rangle \sim \langle V \rangle. \quad (49)$$

The virial theorem is used in the PN expansion for deriving a relationship between the expansion parameters v^2 and G . Thus, due to it being a relationship between time averages, the PN expansion does not really hold point-for-point instead, one has to consider a full orbit.⁵ This is not the case for the PM expansion since the virial theorem is not used in the derivation of the expansion, thus showcasing another of the PM's strengths. Despite this, the virial theorem is still relevant in the PM case.

When calculating the non-expanded, relativistic kinetic energy for the bodies, as is done in this paper, it is important to consider that even though it is only a function of p^2 there are higher orders of p hiding in the Taylor expansion of the square root:

$$E = \sqrt{m^2 c^4 + p^2 c^2} = mc^2 \left(1 + \frac{1}{2} \frac{p^2}{m^2 c^2} - \frac{1}{8} \frac{p^4}{m^4 c^4} + \dots \right). \quad (50)$$

Thus, according to the virial theorem, there will be, for example, effects on the order of G^2 entering the 1PM expansion through the kinetic energy, even after truncating the 1PM EOM by removing all terms with G of higher order than one.

3.5 Analytical expressions for observables

In order to properly analyze the quality of simulated results, one has to be able to compare them to some analytically derived values for known observables. In the two body problem examples of such known observables are the scattering angle, the periastron precession and the eccentricity.

3.5.1 Scattering angle

The scattering angle is defined as the total change in the angular coordinate, experienced during the scattering, minus π radians, as no scattering would leave the change in the radial coordinate equal to π radians. From here on out, the scattering angle will be referred to as $\Delta\theta$. For the Newtonian case one has the well known expression, here taken from [3]:

$$\Delta\theta_N = 2 \arctan \left(\frac{G m_1 m_2}{v_\infty L} \right) \quad (51)$$

where v_∞ is the initial velocity of the scattering body "infinitely" far away and $L = \|\mathbf{r} \times \mathbf{p}\|$ is the angular momentum.

Defining the function $B(\alpha) = \arctan(\alpha) + \frac{\pi}{2}$, where $\alpha = G m_1 m_2 / (v_\infty L)$, the 1PN scattering angle is given in [3] as

$$\Delta\theta_{1\text{PN}} = \Delta\theta_N + 2 \left(\frac{v_\infty \alpha}{c} \right)^2 \left[3B(\alpha) + \frac{3\alpha^2 + 2}{\alpha(1 + \alpha^2)} \right] \quad (52)$$

$$= 2 \arctan(\alpha) + 2 \left(\frac{v_\infty \alpha}{c} \right)^2 \left[3B(\alpha) + \frac{3\alpha^2 + 2}{\alpha(1 + \alpha^2)} \right]. \quad (53)$$

As the PM is a perturbative method in G , the full values of observables, such as the scattering angle, will be a sum of contributions at higher and higher orders

$$\Delta\theta_{\text{PM}} = O(G^1) + O(G^2) + O(G^3) + \dots \quad (54)$$

This structure can be seen in the expressions for the scattering angle in the 1PM and 2PM taken from [7]:

$$\Delta\theta_{1\text{PM}} = \frac{G f_1}{p_0 L} \quad \text{and} \quad \Delta\theta_{2\text{PM}} = \frac{G f_1}{p_0 L} + \frac{G^2 f_2 \pi}{2L^2} \quad (54 \text{ a,b})$$

⁵One can not be completely sure that when looking at a small section of a body's orbit that it is completely "correct"; its general behaviour with respect to full orbits is however, correctly described by the PN expansion.

where the angular momentum $L = bp_\infty$ is dependent on the impact parameter b , and the magnitude of the momentum at infinity. The coefficients in equations (54 a,b) are given by

$$f_1 = -\frac{2c_1}{(E_1 + E_2)/c}, \quad f_2 = -\frac{1}{2(E_1 + E_2)/c} \left(\frac{c_\triangleright}{m_1} + \frac{c_\triangleleft}{m_2} \right), \quad p_0 = \sqrt{\frac{(E_1 E_2/c^2 - p^2)^2 - m_1^2 m_2^2 c^4}{(E_1 + E_2)^2/c^2}}, \quad (55)$$

c_1 , c_\triangleright and c_\triangleleft are as defined in equations (37) and (48 a,b).

3.5.2 Periastron precession

One of the greatest confirmations of the validity of GR is its ability to explain the periastron shift, or precession, of the orbit of the planet Mercury [13]. Unlike Newtonian mechanics predicts, not all isolated orbits are stable ellipses.⁶ Instead, the ellipse slowly rotates in the angular direction around the center of mass of the system (see Figure 8 for example).

In the Newtonian case the precession is thus equal to 0, as previously mentioned:

$$\Delta\phi_N = 0. \quad (56)$$

In both the 1PN and 1PM cases, Robertson's formula for the precession angle (which is to order 1 in G) is used,

$$\Delta\phi_{1\text{PN}} = \Delta\phi_{1\text{PM}} = 6\pi \left(\frac{Gm_1 m_2}{cL} \right)^2, \quad (57)$$

where a is the semi-major axis of the (quasi-Newtonian) relative orbit and e is the eccentricity [9]. One has to be careful though, as these regimes both include special relativistic effects, while the formula doesn't.

For the 2PM expansion, the precession is given by the following formula taken from [8]

$$\Delta\phi_{2\text{PM}} = \frac{3\pi}{2} \left(\frac{Gm_1 m_2}{cL} \right)^2 \frac{E(5\gamma^2 - 1)}{(m_1 + m_2)c^2}, \quad (58)$$

where $E = M\sqrt{1 + 2\nu(\gamma - 1)}$ is the total energy with $M = m_1 + m_2$ and $\nu = m_1 m_2/M^2$. It can be seen that in the limit where $\gamma \rightarrow 1$ then equation (58) reduces to (57).

3.5.3 Eccentricity

The eccentricity of an orbit is defined as

$$e = \sqrt{1 - \frac{b^2}{a^2}}, \quad (59)$$

where a and b are the semi-major and -minor axes, respectively, of the first annual ellipse⁷ of the orbit. The eccentricity is directly related to the angular momentum in the following manner:

$$(1 - e^2)a = \frac{L^2}{GM}. \quad (60)$$

Thus, the scattering and precession angle formulas depend on the eccentricity by extension.

4 Numerical Methods

As seen in the previous chapter, the EOM for higher orders of the PN and PM expansions get very large, and thus, doing the calculations by hand becomes quite unfeasible, as well as it being very difficult to find analytical solutions to the integrals of the EOM. It is therefore common to turn to the power of computers to do the simulation, as they can do the hard work and calculation to any given order of accuracy. In this section the numerical implementation in Python of a TBP simulator is presented.

⁶Precession does occur in Newtonian mechanics when considering, e.g., the combined gravitational effects of all the planets in the solar system on each other. This does, however, not fully explain all of Mercury's precession.

⁷I.e. the (quasi-)ellipse that one mass forms after one "year" of its orbit.

4.1 Units

When simulating any physical problem numerically, it is important to be consistent with ones system of units. The computer does not know kilometers from Coulombs after-all. Given a case of two stellar objects. Their masses could be described in terms of a number of different units, such as the mass of Jupiter or the rest energy of a proton divided by the speed of light squared.

While the choice of units is arbitrary, it makes sense to have units that reflect the scales of the problem. Another thing to take into account is that Pythons floating point numbers⁸ have a limited range of around $\sim 10^{\pm 308}$,⁹ which makes exceedingly large or small numbers a problem in calculations, as they are prone to reach these limits faster in calculations. Thus one wants values that are representative of the problem and which don't stray too far from 0.

When simulating gravity using classical physics and relativity on a solar system to black hole binary type scale, an appropriate choice of units could be

$$[\text{mass}] = M_S, \quad [\text{distance}] = GM_S/c^2, \quad [\text{time}] = GM_S/c^3 \quad (61)$$

with the rest of the units being expressed as a linear combination of these.¹⁰ These three units represent mass in the units of solar masses, distances in units of half the suns Schwarzschild radius, and time in units of the time it takes light to traverse half the Sun's Schwarzschild radius. This is, furthermore, a practical choice for solving the equations from Sections 3.2.1 - 3.3.2, as they all contain the constants G and c which can then be set equal to one when using this choice of units. When giving the values of the problem to the computer, these units are used to *non-dimensionalize*, and then to *re-dimensionalize*, so to speak.

As an example, imagine the Earth orbiting the Sun. The parameters of the problem would be non-dimensionalized as such (here tildes are used for the dimensionless parameters):

$$\tilde{m}_1 = m_1/M_S, \quad \tilde{m}_2 = m_2/M_S, \quad \tilde{r}_{\text{init}} = \frac{r_{\text{init}}}{GM_S/c^2}, \quad \tilde{v}_{\text{init}} = v_{\text{init}}/c \quad (62)$$

where r_{init} and v_{init} are the initial relative distance and initial tangential speed. The program then simulates and returns dimensionless values which are then converted back into SI with the chosen units by inverting this method. In this way one can turn many different physical problems into something digestible for a computer, for it to crunch the numbers. Moreover, when the computer calculates an orbit, it works for all masses $M = \kappa \cdot M_S$:

$$[\text{mass}] = \kappa \cdot M_S, \quad [\text{distance}] = \kappa \cdot GM_S/c^2, \quad [\text{time}] = \kappa \cdot GM_S/c^3 \quad (63)$$

This means that the simulation, in a sense, runs at all scales simultaneously. This is called dynamic similarity and is a great power of numerical simulations.

4.2 Numerically solving the two-body problem

To solve the problem, one must first define the initial state of two bodies. Here, their positions \mathbf{r}_i , momenta \mathbf{p}_i and masses m_i are relevant¹¹

$$\mathbf{s}_0 = [\mathbf{r}_1, \mathbf{p}_1, m_1, \mathbf{r}_2, \mathbf{p}_2, m_2]. \quad (64)$$

Using the results from Section 2.1 one can transform the initial conditions to the center of mass frame

$$\mathbf{s}_0^{\text{CM}} = [\mathbf{r}, \mathbf{p}, m_1, m_2], \quad (65)$$

where $\mathbf{r} = \mathbf{r}_1 - \mathbf{r}_2$ is the relative vector between the bodies and $\mathbf{p} = \mathbf{p}_1^{\text{CM}} = -\mathbf{p}_2^{\text{CM}}$ is their COM momentum (opposite but equal for the bodies).

⁸More can be read on floating points here: <https://www.geeksforgeeks.org/python-float-type-and-its-methods/> (accessed: 02/06/2022).

⁹Found at <https://note.nkmk.me/en/python-sys-float-info-max-min/> (accessed: 01/06/2022).

¹⁰Except for things like Ampere or Coulomb, but these are not relevant in this context.

¹¹Note that it hasn't been specified in which coordinates in which these variables are given.

Now choosing the appropriate model Hamiltonian in the center of mass frame and deriving the EOM in that frame

$$H(\mathbf{p}, \mathbf{r}) \longrightarrow \begin{cases} -\frac{\partial H}{\partial \mathbf{r}} = \dot{\mathbf{p}}, \\ \frac{\partial H}{\partial \mathbf{p}} = \dot{\mathbf{r}}, \\ \frac{d}{dt} \frac{\partial H}{\partial \mathbf{p}} = \ddot{\mathbf{r}}, \end{cases} \quad (66)$$

from which one gets a set of coupled differential equations

$$(i) \quad \frac{d\mathbf{r}}{dt} = \dot{\mathbf{r}} = \mathbf{v}, \quad (ii) \quad \frac{d^2\mathbf{r}}{dt^2} = \ddot{\mathbf{r}} = \mathbf{a}. \quad (67)$$

These can then be iteratively and discretely integrated using an integrator of choice.

The integration will occur within an iterative function \mathcal{I} that takes the states of the system at time t , $s(t)$ and returns the state $s(t + dt)$,

$$\mathcal{I}(s(t)) = s(t + dt), \quad (68)$$

whereby the integrator of choice in this paper will be the `solve_ivp` function from the SciPy Python library. Here it is important to be careful when choosing a method of integration, making sure to have an energy-conserving integrator, for example a symplectic one. Running the iterative function starting at $t = 0$ and up to some final time t_f , will ultimately result in an array of relative positions $[\mathbf{r}]$, that can then be transformed back to arrays of $[\mathbf{r}_1]$ and $[\mathbf{r}_2]$, using equations (2), that will then describe the motion of each body.

Example: Simulating the Earth-Sun system As an example take again the Earth-Sun system; 2 bodies with masses m_1 and m_2 gravitationally bound to each other through a conservative potential $V(r)$. The initial state in the inertial frame centered at the sun is

$$\mathbf{r}_1 = (10^8, 0) \frac{GM_{\text{S}}}{c^2}, \quad m_1 = 3 \times 10^{-6} M_{\text{S}}, \quad \mathbf{p}_1 = (0, 3 \times 10^{-10}) M_{\text{S}} c, \quad (69)$$

$$\mathbf{r}_2 = (0, 0), \quad m_2 = M_{\text{S}}, \quad \mathbf{p}_2 = (0, 0) M_{\text{S}} c, \quad (70)$$

and in the COM frame, the masses are unchanged, but the relative position and COM momentum become

$$\mathbf{r} = (10^8, 0) \frac{GM_{\text{S}}}{c^2} \quad \text{and} \quad \mathbf{p} = (0, 1.5 \times 10^{-10}) M_{\text{S}} c. \quad (71)$$

Using the fact that the orbital motion of these two bodies will be confined to a plane ensures that the coordinate system is situated such that the Hamiltonian will only be a function of two spatial coordinates, instead of three as explained in Section 2.2. Then the Newtonian two-body Hamiltonian in the COM frame becomes

$$H_N(\mathbf{p}, \mathbf{r}) = \frac{1}{2} \left(\frac{1}{m_1} + \frac{1}{m_2} \right) \mathbf{p}^2 - \frac{Gm_1m_2}{r}, \quad (72)$$

and the Hamiltonian equations give

$$\dot{\mathbf{r}} = \frac{\partial H}{\partial \mathbf{p}} = \left(\frac{1}{m_1} + \frac{1}{m_2} \right) \mathbf{p} \quad (73)$$

$$\text{and} \quad \dot{\mathbf{p}} = -\frac{\partial H}{\partial \mathbf{r}} = -\frac{Gm_1m_2}{r^3} \mathbf{r}, \quad (74)$$

from which one can obtain

$$\ddot{\mathbf{r}} = \left(\frac{1}{m_1} + \frac{1}{m_2} \right) \dot{\mathbf{p}} = -\frac{G(m_1 + m_2)}{r^3} \mathbf{r} = \mathbf{a}(t) \quad (75)$$

Specifying the initial conditions \mathbf{r}_0 and \mathbf{p}_0 is then sufficient to determine the subsequent motion at all times t .

To integrate this, one can for example use the first order symplectic Euler integration scheme like this:

$$\mathbf{a}(t) = \mathbf{a}(t) \quad (76)$$

$$\mathbf{v}(t + dt) = \mathbf{v}(t) + \mathbf{a}(t) dt \quad (77)$$

$$\mathbf{r}(t + dt) = \mathbf{r}(t) + \mathbf{v}(t + dt) dt. \quad (78)$$

Now using the results from Section 2.1 to change from the center of mass motion $\mathbf{r}(t)$ to the motion of the two individual bodies and plotting the positions, the result will be something like what is seen in Figure 1.

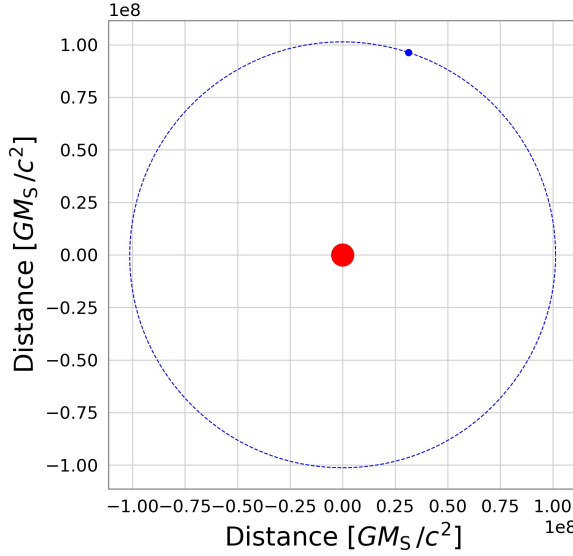


Figure 1: The orbit of the Earth around the Sun. It is seen that the orbit is almost completely circular.

4.3 Extracting parameters from simulations

4.3.1 Scattering angle

The following will be used to calculate the scattering angle from the simulations:

$$\Delta\theta_{\text{simulation}} = \pi - \arccos \left(\frac{(\mathbf{x}_i - \mathbf{b}) \cdot (\mathbf{x}_f - \mathbf{b})}{\|\mathbf{x}_i - \mathbf{b}\| \|\mathbf{x}_f - \mathbf{b}\|} \right) \quad (79)$$

where \mathbf{x}_i and \mathbf{x}_f are the initial and final positions of the test body, and \mathbf{b} is the vector with the magnitude of the impact parameter b pointing in the direction perpendicular to the initial momentum of the test body \mathbf{p} , which is subtracted from \mathbf{x}_i and \mathbf{x}_f in order to move the point of closest approach to the origo.

4.3.2 Periastron precession

To extract the periastron shift $\Delta\phi$ of one of the masses m_1 in a given simulation, its distance from the center r_1 is extracted for each time giving an array of distances as a function of time (see Figure 2).

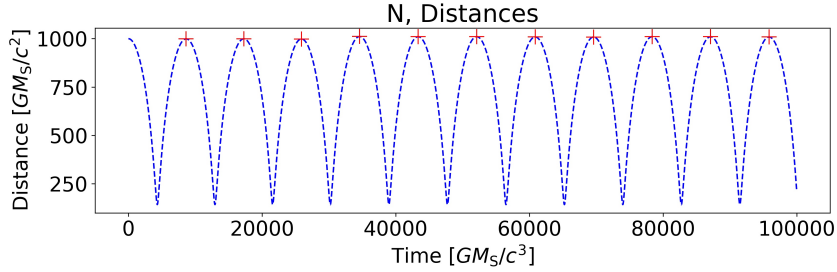


Figure 2: Plot of the distances of the test-body to the centre of mass with respect to time shown in blue. The points of furthest distance for each year are shown in red.

Afterwards the peaks of these distance arrays are found, to indicate the positions of each completed orbit. Subsequently the formula for the angle between two vectors is used to find the angle between each consecutive pair of peaks

$$\theta_{ab} = \arccos \left(\frac{\mathbf{a} \cdot \mathbf{b}}{ab} \right) \quad (80)$$

Thus one ends up with an array of the periastron shifts between each consecutive year. (see Figure 8).

5 Results

Having derived the EOM for a binary system in various expansions, one can now simulate and analyze the system. This will mainly consist of analyzing parameters in bound and scattering states for all expansions.

5.1 Scattering systems

The scattering system captures the scenario of two rogue objects encountering each other with energies too high to actually end up in a bound state, but still passing close enough to exert meaningful gravitational forces on each other. In scattering, there are two meaningful parameters; the momentum before the gravitational attraction takes place p_∞ and the impact parameter b defined as the distance of closest approach where the two objects continue in straight lines. This section looks at scattering for systems in the test-body limit with the same impact parameter b but varying initial momentum p_∞ , thus varying angular momentum $L = bp_\infty$.

5.1.1 Ultra-relativistic scattering

As mentioned before, one of the PM expansion's main strengths lies within the regime of ultra-relativistic scattering, $v \lesssim c$ [5]. This can be seen in Figure 3 with $v = 0.9c$, where the difference between the analytical and simulated values for 1PN is around 1.15° or 31% while for the PM expansions it is around 0.06° or 2%. The Newtonian simulation returns a value consistent with its analytical expression.

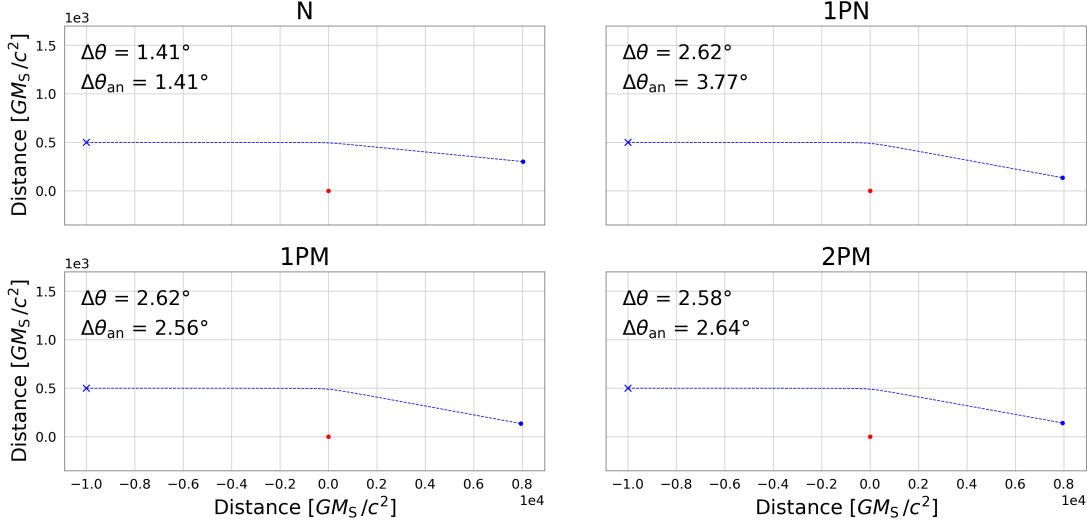


Figure 3: Ultra-relativistic scattering in test-body limit at $v = 0.9c$ for Newtonian case, 1PN, 1PM and 2PM.

5.1.2 Non-relativistic scattering

For the scattering test with non-relativistic velocity, $v = 0.2c$ it is seen in Figure 4 that the simulated scattering angle of the 1PM actually comes closest to its respective analytical value, with a difference of 0.18° or around 0.6% , while the maximum deviance, of 2.25° or around 8% , is observed for the 1PN simulation. The Newtonian then has a difference of 0.85° or around 3% and the 2PM has a difference of 1.55° or around 5% .

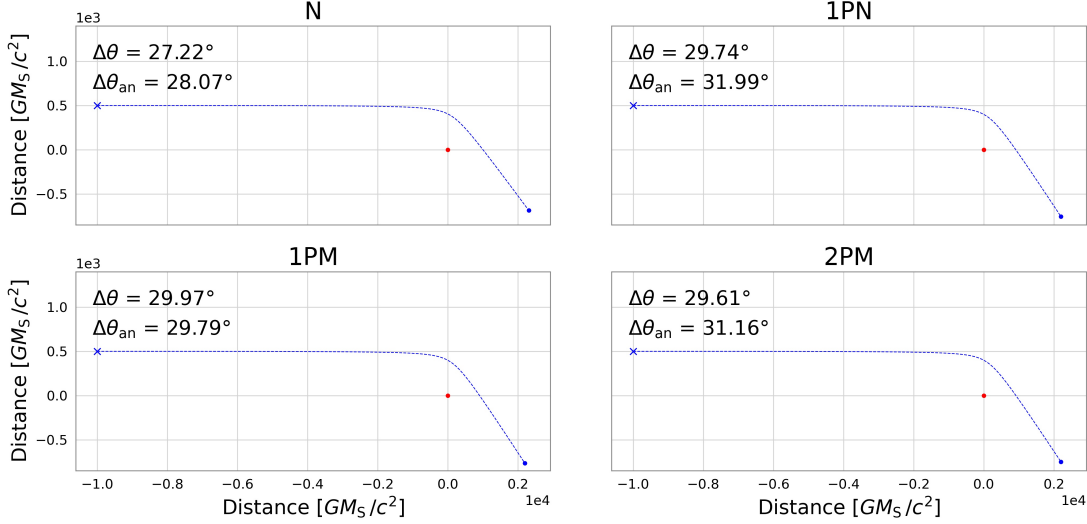


Figure 4: Non-relativistic scattering in test-body limit at $v = 0.2c$ for Newtonian case, 1PN, 1PM and 2PM.

5.1.3 Scattering angle vs angular momentum

Considering how the validity of the PN and PM expansions differ between velocity regimes, it is of interest to see the effect of varying this parameter. The relationship between scattering angle and angular momentum

at velocities between $0.3c \leq v \leq 0.9c$ can be seen in Figures 5 and 6. The latter has a close-up comparison of the 1PN, 1PM and 2PM expansions on the left, showing how the 1PM is slightly larger than the 2PM for the simulation while the opposite is true for the analytical values. The simulated values for the 1PN lie in between that of 1PM and 2PM (interestingly coinciding perfectly with the analytical values for the 2PM) but the analytical values of the 1PN are higher than all of the other values. Of the three, the 2PM simulation is in closest agreement with its corresponding analytical calculations, as can be seen on the right in Figure 6, with a difference on the order of 0.1° . The 1PN scattering angle, again, has the largest difference of around 1.5° while the 1PM converges towards a value of around 0.2° but is observed to be as high as approximately 0.8° in the low angular momentum limit. The Newtonian simulation is in near perfect agreement with analytics.

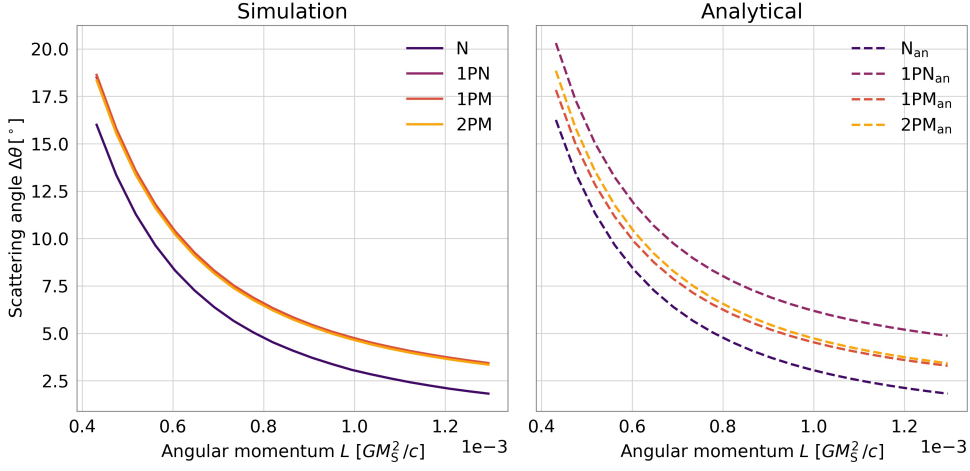


Figure 5: Scattering angle as a function of angular momentum, simulated on the left and analytical results on the right, for Newtonian case, 1PN, 1PM and 2PM.

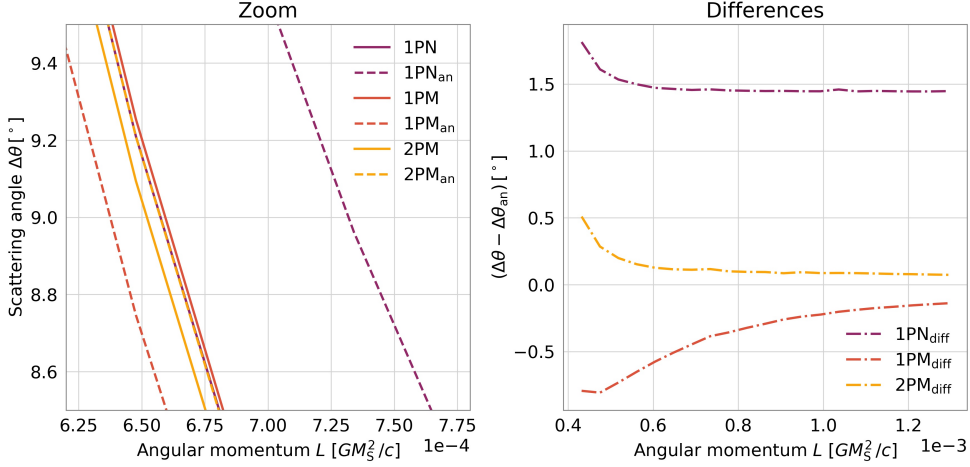


Figure 6: On the left: Zoomed in section of combination of the plots from Figure 5. On the right: Plot of the differences between simulated and analytical scattering angles as a function of angular momentum, for 1PN, 1PM and 2PM.

5.2 Bound systems

Bound state systems are systems where two masses orbit their mutual center of mass, and both orbits are then characterized by their elliptical (in the Newtonian case) or quasi-elliptical forms. Examples of bound systems are abundant within the universe, as all solar systems have planets and asteroids bound to the parent star(s) and moons bound to their respective planets. An important parameter of a bound state system is its eccentricity and angular momentum. This section uses the traditional definition of angular momentum, $\mathbf{L} = \mathbf{r} \times \mathbf{p}$, varying the momentum to probe the behaviour of the precession.

5.2.1 Non-eccentric similar mass binary system

The case of a non-eccentric orbit of similarly massive objects portrays a system of two stars, neutron stars or black-holes orbiting each other. As the two objects are of similar masses, their center of mass, which they both orbit, will be right in between them, and thus the trajectories should be 2 circles whose radii obey the simple relation $R_1/R_2 = m_1/m_2$. In Figure 7 it is seen that the simulation exhibits this expected behaviour in all four cases.

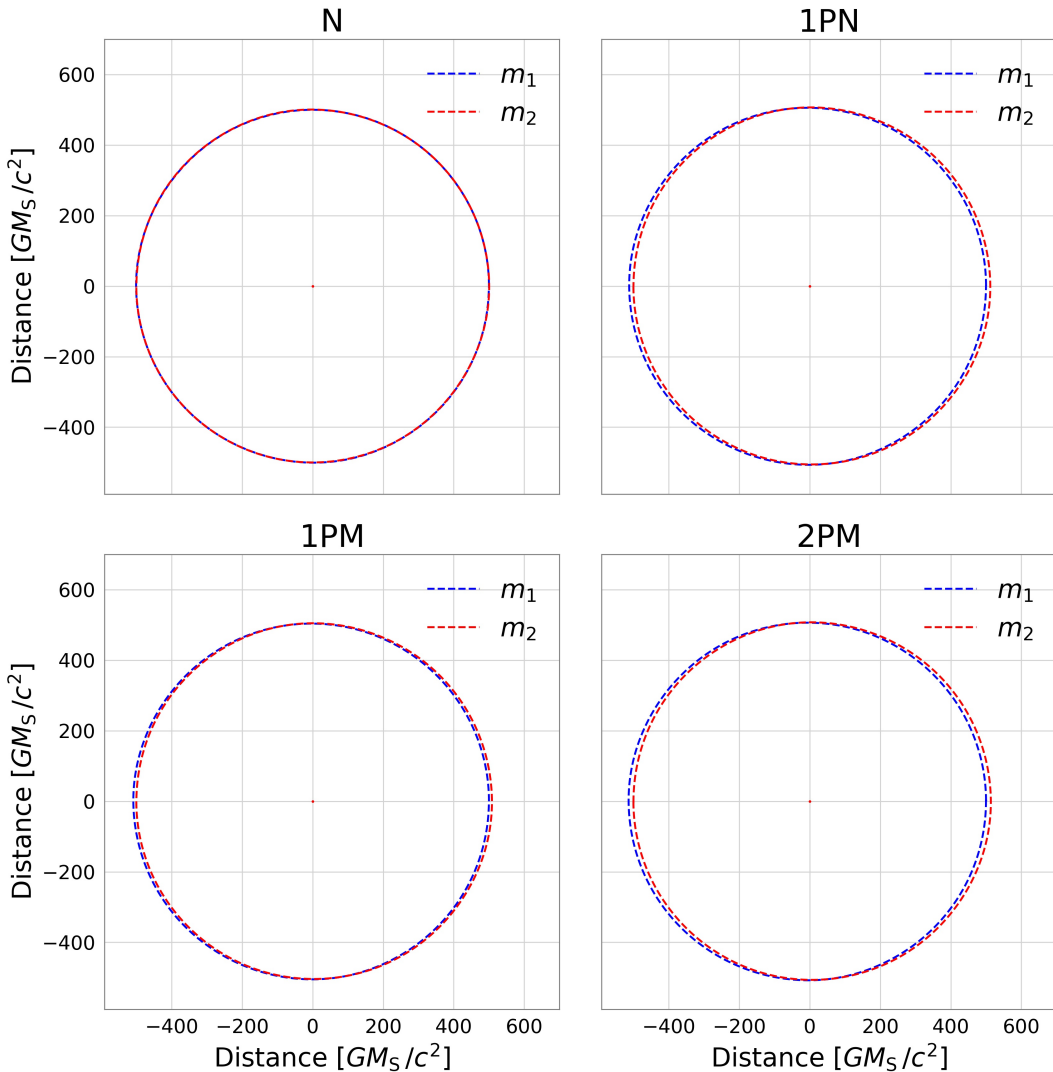


Figure 7: Non-eccentric similar mass binary system for Newtonian case, 1PN, 1PM and 2PM, with $m_1 = m_2$.

5.2.2 Precession in eccentric test-body limit

The case of an eccentric orbit of a small mass around a much larger mass portrays a system of a small mass orbiting a larger mass, for example, Mercury's orbit around the sun, although Mercury's precession is very small, so another, more eccentric system has been chosen to better illustrate the shift. In Figure 8 it can be seen how no precession occurs in the Newtonian case which agrees with the analytical value. All three GR cases exhibit precession with the 2PM case being in closest agreement with its analytical value, having a difference of less than a tenth of a degree. The 1PN precession angle differs from its analytical value by 0.1° or 2%, while the 1PM has the highest discrepancy, of 0.8° or 19%.

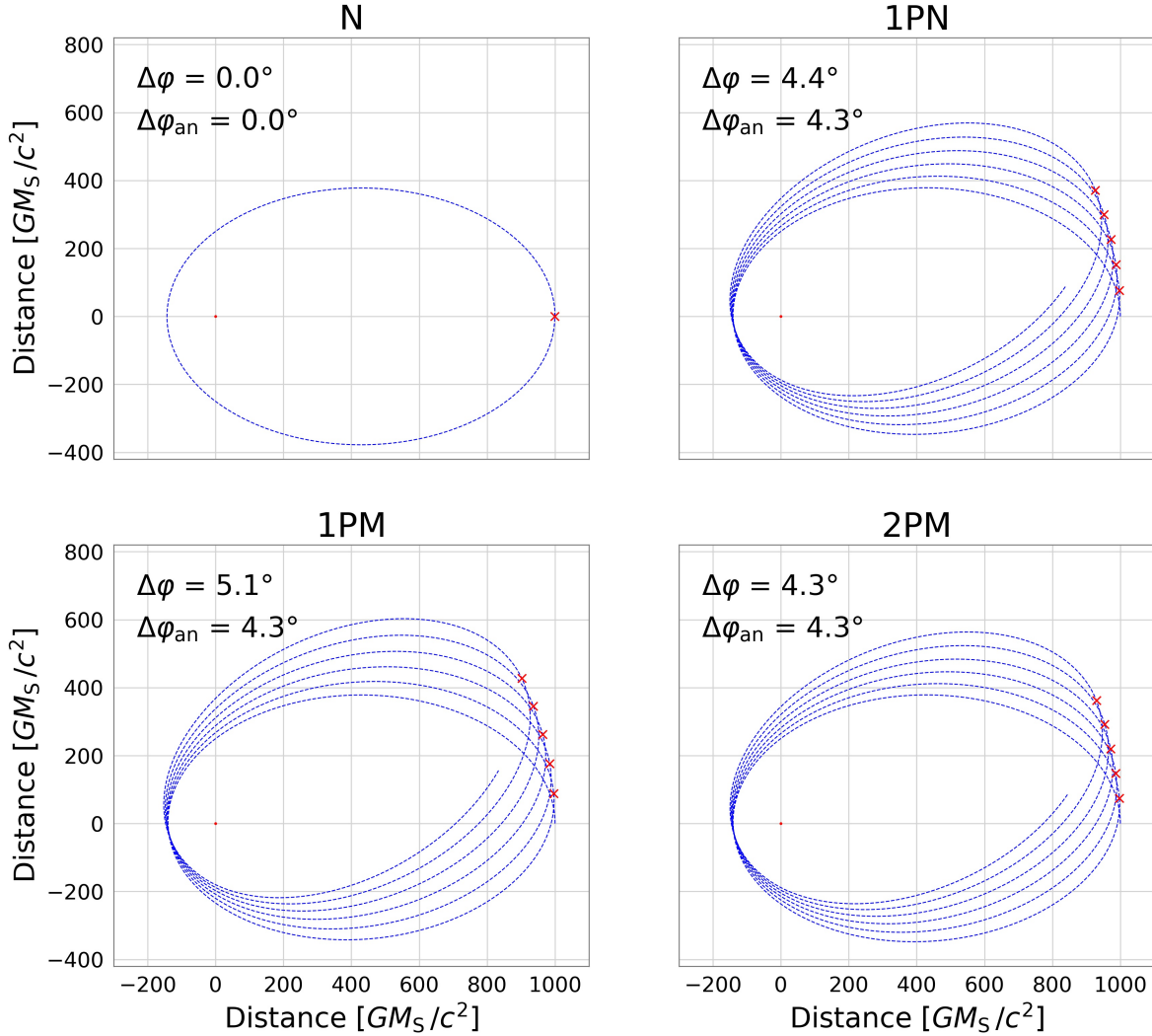


Figure 8: Precession in eccentric test-body limit for Newtonian case, 1PN, 1PM and 2PM.

5.2.3 Precession in eccentric similar mass binary system

The case of an eccentric orbit of two similarly massive objects portrays the eccentric version of the system in Section 5.2.1 but with non-equal masses. Figure 9 displays similar behaviour as for the precession in the test-body limit. There is no precession in the Newtonian case while the 1PN has a difference of 1.7° or around 11%, the 1PM 3.2° or 21% and the 2PM 1.6° or 11%.

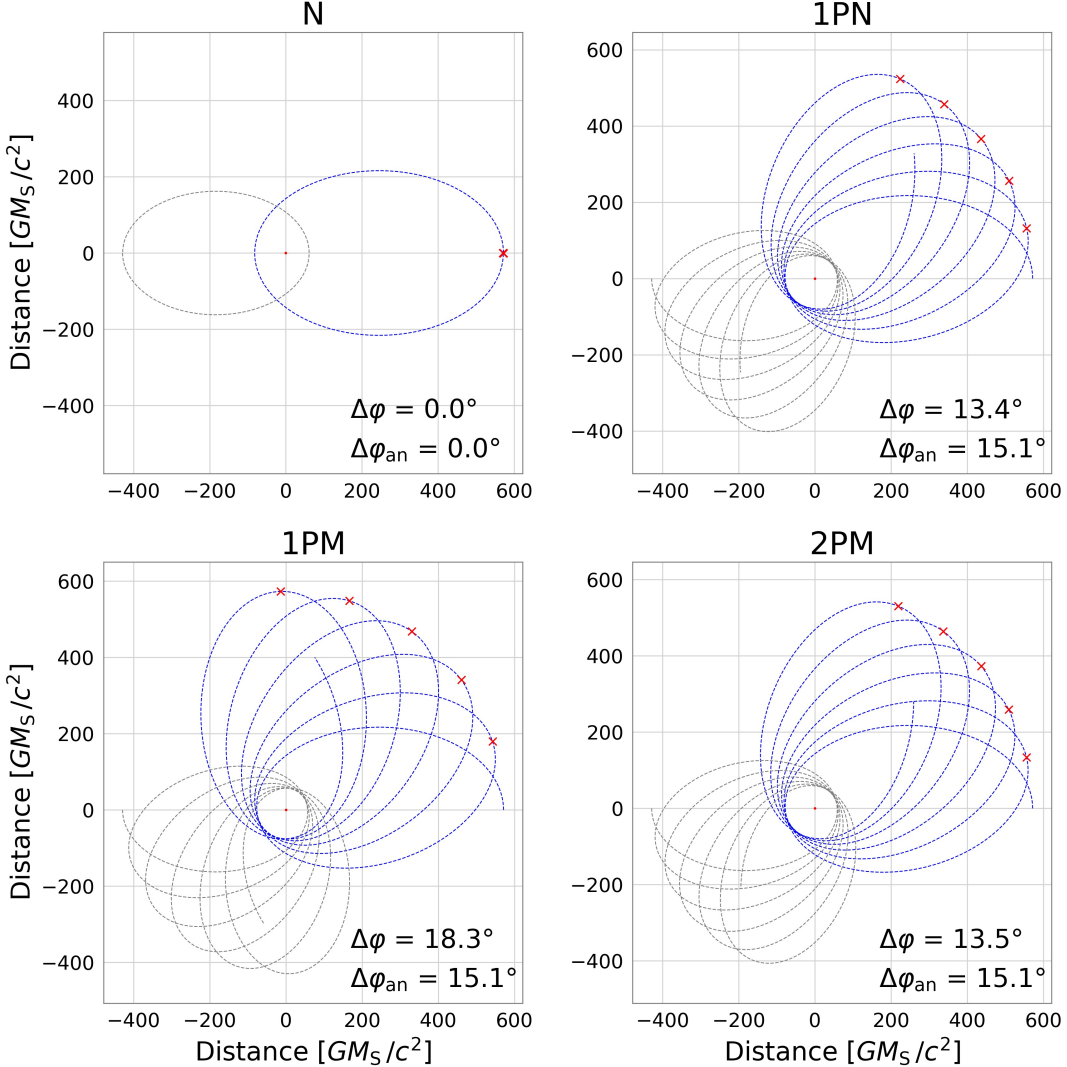


Figure 9: Precession of one object in eccentric similar mass binary system for Newtonian case, 1PN, 1PM and 2PM.

5.2.4 Precession angle vs angular momentum

In Figure 10 it is seen that the precession angle depends on the angular momentum in a similar way as the scattering angle. In both simulations it can be seen that the Newtonian case has precisely 0 precession, which agrees with the analytical prediction. In Figure 11 it is seen in all cases of both simulations that the deviance from the analytical value is greatest for low angular momentum. All of the expansions for both simulations converge to zero for high angular momentum, although the 1PM does so slower than the others.

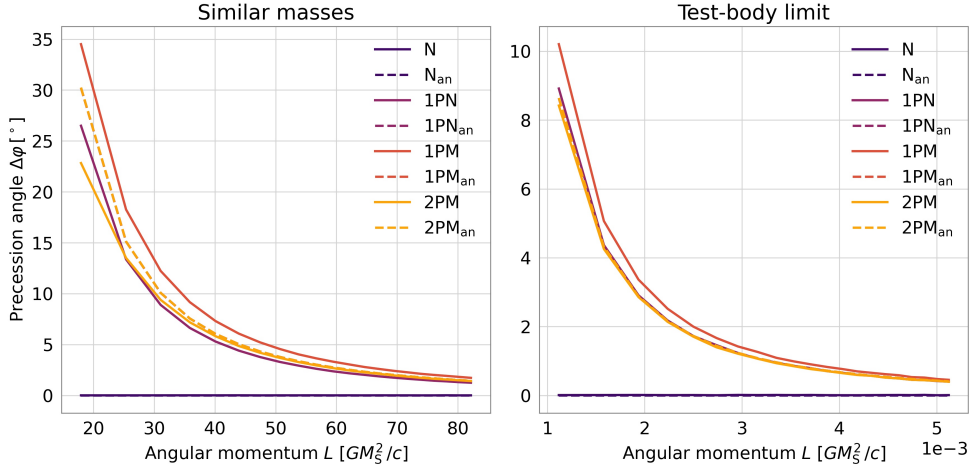


Figure 10: Two plots of the simulated and analytical precession angles as a function of angular momentum in both the eccentric similar mass and test-body cases.

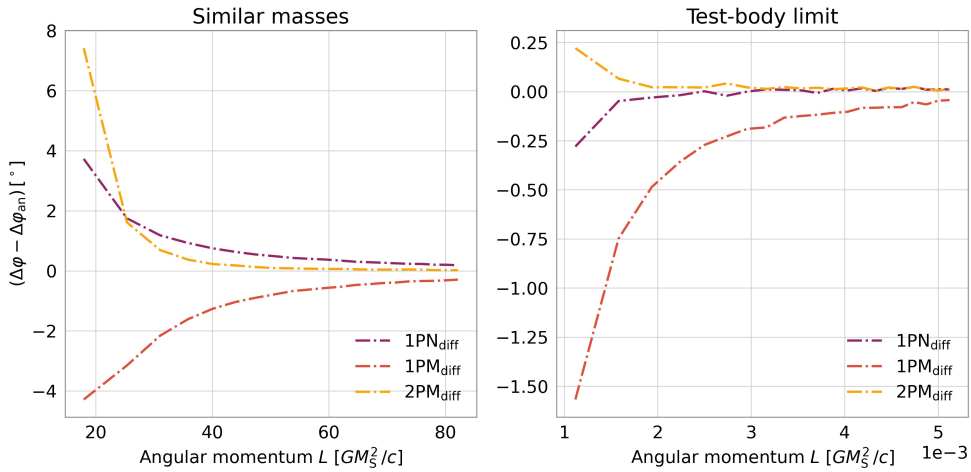


Figure 11: Plot of the differences between simulated and analytical precession angles as a function of angular momentum, for both similar mass case and test-body limit for 1PN, 1PM and 2PM.

5.2.5 Relativistic Newtonian orbits

In light of the discussion in Section 3.4.2, an interesting experiment to perform is to make a so-called relativistic Newtonian simulation, i.e. derive equations of motion using a Hamiltonian consisting of special relativistic kinetic energies and a classical Newtonian potential:

$$H_{N_{rel}} = E_1 + E_2 - \frac{Gm_1m_2}{r} \quad (81)$$

where $E_i = \sqrt{m_i^2c^4 + p^2c^2}$ in the center of mass frame. Figure 12 shows results of an experiment of this kind where the relativistic Newtonian orbit is seen to have a precession angle of 4.0° .

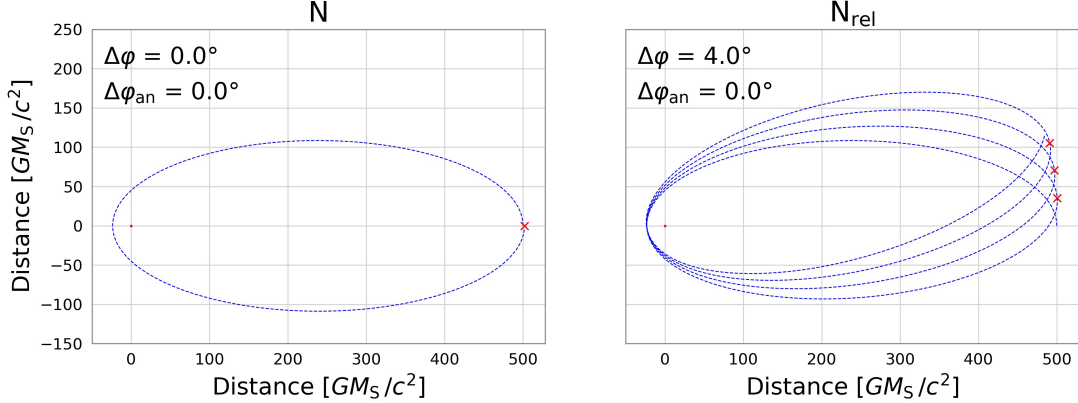


Figure 12: Classical Newtonian orbit compared with relativistic Newtonian orbit with precession.

5.3 Conservation of energy and angular momentum

The PN and PM expansions discussed in this paper do not have radiative effects due to being at low enough order, i.e. the systems are conservative. Here, the total energy and angular momentum within the simulations are examined. Figure 14 shows these as functions of time for the bound state test-body limit, where the total energy has been calculated using the respective Hamiltonians. The figure shows fluctuations of the energies of order less than 10^{-6} and of order less than 10^{-2} for angular momentum.

A deconstruction of the total energy for the 2PM case from Figure 14 into potential and kinetic energy is shown in Figure 13. Both energies exhibit fluctuations, but in opposite directions, of similar magnitude.

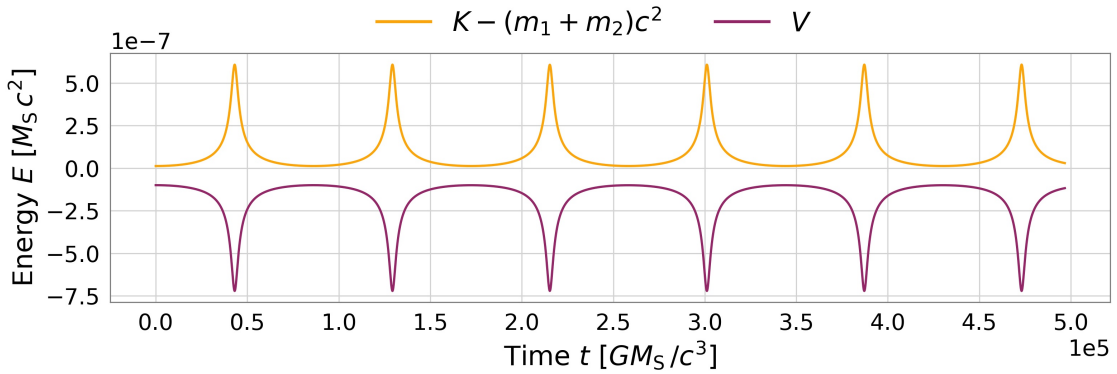


Figure 13: Plot of the 2PM potential energy and 2PM kinetic energy minus the rest mass energy in the eccentric test-body limit case.

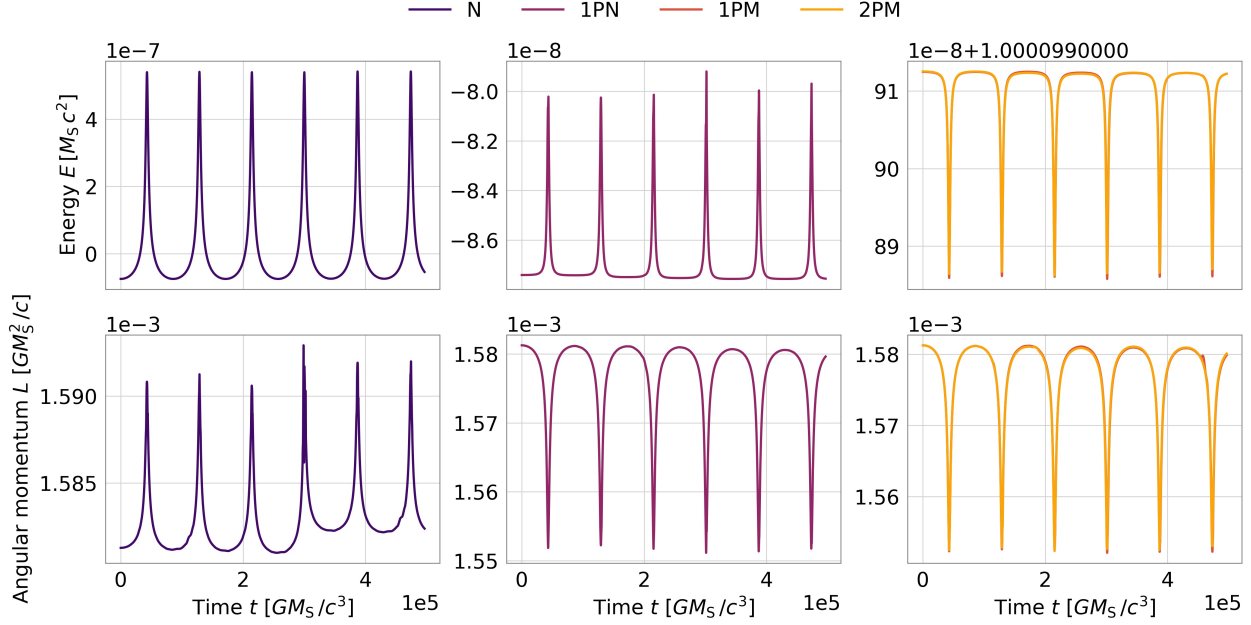


Figure 14: Energy and angular momentum as a function of time for Newtonian, 1PN, 1PM and 2PM cases in the eccentric test-body case. The 1PM and 2PM energies and angular momenta are plotted together in the third column on the right and coincide near perfectly.

6 Conclusions and Further Work

In the plots showing the energy and angular momenta as a function of time in the eccentric test-body case, it would appear, at first glance, that the energy and angular momentum are not conserved. Upon further inspection, however, one sees that the variations are very small, around $10^{-7} \cdot M_S c^2$ and $10^{-8} \cdot M_S c^2$ for the energies. When taking into account that the masses used in all the simulations are $1 \cdot M_S$, giving a rest mass energy of $E = 1 \cdot M_S c^2$ which is equal to 1 in the units used throughout the paper, it is clear that these fluctuations can safely be ignored. For all scattering and bound state cases similar behaviour was observed.

The figure containing the kinetic and potential energies for the eccentric test-body case, shows how these have synchronous peaks of similar magnitude pointing in opposite directions; the kinetic peaking and the potential dipping where the orbiting body is closest to the big body. It is seen that the peaks coincide with the fluctuations in total energy, therefore, it is likely that these fluctuations are merely the result of numerical errors being more pronounced in these extreme regions. I.e. the magnitudes of the peaks not matching perfectly and thus giving tiny, but non-zero fluctuations when subtracted from each other. Again, similar behaviour was observed for all scattering and bound state cases.

The results presented in Section 5.1 confirm the suspicion that the 1PM and 2PM expansions are superior to the 1PN expansion and the Newtonian case in the ultra-relativistic regime, that is for velocities approaching the speed of light. This is illustrated by the 31% inaccuracy of the 1PN with respect to the analytical value in the ultra-relativistic case, while the Newtonian, 1PM and 2PM cases have a maximum inaccuracy of around 2%. To further this point, it can be seen that in the non-relativistic limit, the relative inaccuracy of all cases are around the same order $\sim 1\%$, except for the 1PN which is around $\sim 10\%$, i.e. the 1PN performs better in this limit compared to the ultra-relativistic limit; but still performs worse than the others cases. The reason for this could be the fact that the 1PN is an expansion in the velocity around zero, thus making it formally invalid in the ultra-relativistic regime.

It should be pointed out that although the Newtonian simulation is consistent with its analytical value, it differs the most from the 2PM analytical value, which theoretically encapsulates more of the actual

physics because of the inclusion of higher order correction terms. Thus, the Newtonian simulation must be theoretically farthest from the true physical reality, which is to be expected since the motivation behind general relativity was finding a more accurate description of reality.

For the figure illustrating the scattering angle as a function of angular momentum one sees the 2PM in close agreement with its analytical values and the 1PN agreeing the least. It is also seen that the Newtonian values are generally lower than the corrected cases. This makes sense, since the Newtonian equations don't include the extra correction terms at small distances that go in to the equations of the expansions (i.e. the terms like $G^2 M/r^2 c^4$, $G^4 M/r^4 c^8$, etc.), and thus the Newtonian motion is less affected in scattering.

Precession was observed in all of the eccentric bound state simulations for 1PN, 1PM and 2PM expansions. The precession is larger for similar mass systems than the test-body limit, which makes sense since the precession angle is a function of the sum of the masses, $m_1 + m_2$, and the masses used in the similar mass simulation were both of the same size as the large mass in the test-body limit, rendering the sum a factor of 2 larger. The amount of precession for 1PN and 2PM is very similar in both simulations and this is likely due to G^2 effects in both expansions, as can be seen in Table 1. Precession is largest for the 1PM expansions which indicates that the higher order correction terms appearing in 1PN and 2PM negate some of the contribution to precession coming from lower order terms.

It should be noted that in both types of bound state simulations, the analytical values are nearly the same for all GR cases, the 1PN and 1PM analytical values being calculated with the same expression (for lack of an alternative in the 1PM case) while the 2PM analytical expression converges to the same value in the non-relativistic limit.

In regards to the non-eccentric similar mass case, which yields circular orbits, the Robertson formula for the precession in this limit actually returns a non-zero value

$$\lim_{e \rightarrow 0} \frac{6\pi G(m_1 + m_2)}{a(1 - e^2)c^2} = \frac{6\pi G(m_1 + m_2)}{ac^2}. \quad (82)$$

The reason that the precession for this case hasn't been explored is because it is hard to define the precession for something that's completely rotationally symmetric. The interpretation could be, that the orbital time predicted by for example Kepler's 3rd law, is maybe shortened by a constant due to this constant precession along the circular path, speeding up the orbiting object.

When comparing the differences between simulated and analytical values for scattering and precession angles as a function of angular momentum, a divergence is seen in both circumstances for $L \rightarrow 0$. Since angular momentum is proportional to distance, this divergence can be interpreted as the effects of strong gravity (happening at small distances), lying outside the regimes of validity for the PN and PM expansions.

One might be tempted to assume that one should not get precession for the 1PM expansion, since it should not include any terms of order G^2 or higher. This is, however, not entirely the case, as was hinted at in Section 3.4.2 regarding the virial theorem, where it was demonstrated that terms on the order of G^2 and higher enter into the equations of motion due to the simulations using the relativistic kinetic energies, which include all orders of p^2 in its expansion, see equation (50). Section 5.2.5, regarding the relativistic Newtonian orbits where the same non-expanded relativistic kinetic energies are used in a simulation with a Newtonian potential, demonstrates this further by yielding precession where one would, otherwise, not have expected it. This is also why the same formula for the precession has been used for both the 1PN and 1PM cases.

Results such as these highlight how the behaviour of the post-Minkowskian expansion can be deceiving and go against intuition. Intuition that is perhaps skewed in favour of the PN expansion due to it having been the gold-standard of general relativistic two-body calculations and simulations for so long.

Further Work

As has been argued, the PM expansion is considerably better than the PN expansion in the regime of ultra-relativistic scattering. Thus, by adding the appropriate energy-dissipative terms to the Hamiltonian, and modelling the energy dissipation in these high energy cases, one could try and predict the character

of gravitational wave signals from binary systems to aid in further gravitational wave observations and discoveries, especially in the case of ultra-relativistic scattering.

Furthermore one could use statistical methods to approximate the distribution of binary systems (bound, scattering or otherwise) throughout the universe and use this to predict a "Gravitational Wave Background", which, if detected at a gravitational wave observatory could provide further insight to the distribution of energy and mass in the universe, revealing potential truths about things like for example dark matter.

Studies of gravitational wave signals, could also give insight into the quantum nature of spacetime, and maybe help unify the theory of General Relativity and Quantum Mechanics and bring us one step closer to a unified theory.

It is evident throughout the paper that when including the non-expanded expressions for the relativistic kinetic energies, one has to be careful. The effects of the higher order terms that enter the EOM due to these expressions, can have unforeseen consequences on the motion. This can be circumvented by properly truncating both higher order potential and kinetic terms when deriving the EOM and would therefore be a prime way of extending the work done in this paper.

As of this paper, the code only runs for exactly two bodies. When it runs through every time-step it references the two bodies and calculates their mutual accelerations. One could potentially have the code run over each body, and then calculate its combined acceleration as a linear combination of the accelerations of all $N - 1$ other bodies in the simulation. Simulating N bodies simultaneously is called the N -body problem, and its implementation would have a structure like

```
for t in arrayOfTimes:
    for currentBody in arrayOfBodies:
        a = (0, 0)
        for otherBody in arrayOfBodies:
            if otherBody != currentBody:
                a += calculateAcceleration(currentBody, otherBody)
        move(a)
```

This would allow for the inclusion of an unlimited amount of bodies in the simulation, bringing it closer to factual reality, but at great cost of efficiency, as adding just one more body leads to an exponential increase in calculations.

One way to combat this inefficiency could be to modify the code such that the time step size, dt , is a function of the distance to the closest mass, and the velocity of the current mass, as this would greatly increase the efficiency of the calculations of far away and slow moving bodies, but keep the wanted level of detail for close, fast moving bodies. Additionally the code could check how close the other bodies are, and then only calculate the acceleration of bodies "nearby".

Bibliography

- [1] Abbott, Benjamin P. et al. "Observation of gravitational waves from a binary black hole merger". In: *Physical review letters* 116.6 (2016).
- [2] Bern, Zvi et al. "Black hole binary dynamics from the double copy and effective theory". In: *Journal of High Energy Physics* 2019.10 (2019).
- [3] Bini, Donato and Damour, Thibault. "Gravitational scattering of two black holes at the fourth post-Newtonian approximation". In: *Physical Review D* 96.6 (2017).
- [4] Blanchet, Luc. "Gravitational radiation from post-Newtonian sources and inspiralling compact binaries". In: *Living Reviews in Relativity* 17.1 (2014).
- [5] Blanchet, Luc. "Analytic approximations in GR and gravitational waves". In: *International Journal of Modern Physics D* 28.06 (2019).
- [6] Carroll, Sean M. *Spacetime and geometry*. Pearson Education Limited, 2014.
- [7] Cristofoli, Andrea et al. "Post-Minkowskian Hamiltonians in general relativity". In: *Physical Review D* 100.8 (2019).
- [8] Damgaard, Poul H and Vanhove, Pierre. "Remodeling the effective one-body formalism in post-Minkowskian gravity". In: *Physical Review D* 104.10 (2021).
- [9] Damour, Thibault and Schäfer, G. "Higher-order relativistic periastron advances and binary pulsars". In: *Il Nuovo Cimento B (1971-1996)* 101.2 (1988).
- [10] Einstein, Albert. "Approximative integration of the field equations of gravitation". In: *Sitzungsber. Preuss. Akad. Wiss. Berlin (Math. Phys.)* 1916.688-696 (1916).
- [11] Fetter, Alexander L. and Walecka, John Dirk. *Theoretical Mechanics of Particles and Continua*. Dover Publications, Inc., 2003. ISBN: 9780486432618.
- [12] Fratus, Keith. *The Two-Body Problem*. URL: <https://web.physics.ucsb.edu/~fratus/phys103/LN/TBP.pdf>. (accessed: 06/05/2022).
- [13] Harmark, Troels. *General Relativity and Cosmology*. 2021.
- [14] Iwasaki, Yoichi. "Quantum theory of gravitation vs. classical theory: fourth-order potential". In: *Progress of Theoretical Physics* 46.5 (1971).
- [15] Morin, David. *The Hamiltonian Method*. URL: <https://scholar.harvard.edu/files/david-morin/files/cmchap15.pdf>. (accessed: 24/05/2022).
- [16] *Post-Minkowskian expansion*. URL: https://en.wikipedia.org/wiki/Post-Minkowskian_expansion. (accessed: 01/06/2022).
- [17] *The Two-body problem*. URL: https://en.wikipedia.org/wiki/Two-body_problem. (accessed: 25/05/2022).
- [18] Will, Clifford M. "On the unreasonable effectiveness of the post-Newtonian approximation in gravitational physics". In: *Proceedings of the National Academy of Sciences* 108.15 (2011).

A Post-Minkowskian Equations of Motion

The EOM from the first three terms of the Hamiltonian in 46 have already been calculated in Section 3.3.1. This section will, therefore, only show the derivations of the $V_{2\text{PM}}$ term using the same definitions as in equations 43 - 45 along with:

$$c_{\triangleright} = 3m_1^2 \left(m_1^2 m_2^2 c^4 - 5 \left(\frac{E_1 E_2}{c^2} + p^2 \right)^2 \right) \quad (83)$$

$$c_{\triangleleft} = 3m_2^2 \left(m_1^2 m_2^2 c^4 - 5 \left(\frac{E_1 E_2}{c^2} + p^2 \right)^2 \right) \quad (84)$$

$$\frac{\partial c_{\triangleright}}{\partial \mathbf{p}} = -30m_1^2 \left(\frac{E_1 E_2}{c^2} + p^2 \right) \left(\frac{1}{c^2} \left(\frac{\partial E_1}{\partial \mathbf{p}} E_2 + E_1 \frac{\partial E_2}{\partial \mathbf{p}} \right) + 2\mathbf{p} \right) \quad (85)$$

$$\begin{aligned} \frac{d}{dt} \frac{\partial c_{\triangleright}}{\partial \mathbf{p}} &= -30m_1^2 \left[\left(\frac{\dot{E}_1 E_2 + E_1 \dot{E}_2}{c^2} + 2\mathbf{p} \cdot \dot{\mathbf{p}} \right) \left(\frac{1}{c^2} \left(\frac{\partial E_1}{\partial \mathbf{p}} E_2 + E_1 \frac{\partial E_2}{\partial \mathbf{p}} \right) + 2\mathbf{p} \right) \right. \\ &\quad \left. + \left(\frac{E_1 E_2}{c^2} + p^2 \right) \left(\frac{1}{c^2} \left(\frac{d}{dt} \frac{\partial E_1}{\partial \mathbf{p}} E_2 + \frac{\partial E_1}{\partial \mathbf{p}} \dot{E}_2 + \dot{E}_1 \frac{\partial E_2}{\partial \mathbf{p}} + E_1 \frac{d}{dt} \frac{\partial E_2}{\partial \mathbf{p}} \right) + 2\dot{\mathbf{p}} \right) \right] \end{aligned} \quad (86)$$

$$\dot{c}_{\triangleright} = -30m_1^2 \left(\frac{E_1 E_2}{c^2} + p^2 \right) \left(\frac{\dot{E}_1 E_2 + E_1 \dot{E}_2}{c^2} + 2\mathbf{p} \cdot \dot{\mathbf{p}} \right). \quad (87)$$

Here $c_{\triangleleft} = m_2^2/m_1^2 c_{\triangleright}$ will be used for simplification.

Thus:

$$\begin{aligned} -\frac{\partial V_{2\text{PM}}}{\partial \mathbf{r}} &= \frac{G^2}{r^4} \frac{2\mathbf{r}}{E_1 E_2} \left[\frac{1}{4c^2} \left(\frac{c_{\triangleright}}{m_1} + \frac{c_{\triangleleft}}{m_2} \right) \right. \\ &\quad \left. + \frac{c_1(E_1 + E_2)}{E_1 E_2} \left(\frac{c_1}{2} \left(\frac{1}{(E_1 + E_2)^2} - \frac{1}{E_1 E_2} \right) - \frac{4}{c^2} \left(\frac{E_1 E_2}{c^2} + p^2 \right) \right) \right] \end{aligned} \quad (88)$$

$$\begin{aligned} \frac{\partial V_{2\text{PM}}}{\partial \mathbf{p}} &= \frac{G^2}{E_1 E_2 r^2} \left\{ -\frac{\frac{\partial E_1}{\partial \mathbf{p}} E_2 + E_1 \frac{\partial E_2}{\partial \mathbf{p}}}{E_1 E_2} \right. \\ &\quad \cdot \left[\frac{1}{4c^2} \left(\frac{c_{\triangleright}}{m_1} + \frac{c_{\triangleleft}}{m_2} \right) + \frac{c_1(E_1 + E_2)}{E_1 E_2} \left(\frac{c_1}{2} \left(\frac{1}{(E_1 + E_2)^2} - \frac{1}{E_1 E_2} \right) - \frac{4}{c^2} \left(\frac{E_1 E_2}{c^2} + p^2 \right) \right) \right] \\ &\quad + \frac{1}{4c^2} \left(\frac{1}{m_1} + \frac{m_2}{m_1^2} \right) \frac{\partial c_{\triangleright}}{\partial \mathbf{p}} \\ &\quad + \left[\frac{E_1 + E_2}{E_1 E_2} \frac{\partial c_1}{\partial \mathbf{p}} + \frac{c_1}{E_1 E_2} \left(\frac{\partial E_1}{\partial \mathbf{p}} + \frac{\partial E_1}{\partial \mathbf{p}} - \frac{E_1 + E_2}{E_1 E_2} \left(\frac{\partial E_1}{\partial \mathbf{p}} E_2 + E_1 \frac{\partial E_2}{\partial \mathbf{p}} \right) \right) \right] \\ &\quad \cdot \left(\frac{c_1}{2} \left(\frac{1}{(E_1 + E_2)^2} - \frac{1}{E_1 E_2} \right) - \frac{4}{c^2} \left(\frac{E_1 E_2}{c^2} + p^2 \right) \right) \\ &\quad + \frac{c_1(E_1 + E_2)}{E_1 E_2} \left[\frac{1}{2} \frac{\partial c_1}{\partial \mathbf{p}} \left(\frac{1}{(E_1 + E_2)^2} - \frac{1}{E_1 E_2} \right) + \frac{c_1}{2} \left(-2 \frac{\frac{\partial E_1}{\partial \mathbf{p}} + \frac{\partial E_2}{\partial \mathbf{p}}}{(E_1 + E_2)^3} + \frac{\frac{\partial E_1}{\partial \mathbf{p}} E_2 + E_1 \frac{\partial E_2}{\partial \mathbf{p}}}{E_1^2 E_2^2} \right) \right. \\ &\quad \left. - \frac{4}{c^2} \left(\frac{1}{c^2} \left(\frac{\partial E_1}{\partial \mathbf{p}} E_2 + E_1 \frac{\partial E_2}{\partial \mathbf{p}} \right) + 2\mathbf{p} \right) \right] \right\} \end{aligned} \quad (89)$$

$$\begin{aligned}
\frac{d}{dt} \frac{\partial V_{2\text{PM}}}{\partial \mathbf{p}} = & - \left(2 \frac{\dot{r}}{r} + \frac{\dot{E}_1 E_2 + E_1 \dot{E}_2}{E_1 E_2} \right) \frac{\partial V_{2\text{PM}}}{\partial \mathbf{p}} \\
& + \frac{G^2}{E_1 E_2 r^2} \left\{ - \left[\frac{\frac{d}{dt} \frac{\partial E_1}{\partial \mathbf{p}} E_2 + \frac{\partial E_1}{\partial \mathbf{p}} \dot{E}_2 + \dot{E}_1 \frac{\partial E_2}{\partial \mathbf{p}} + E_1 \frac{d}{dt} \frac{\partial E_2}{\partial \mathbf{p}}}{E_1 E_2} - \frac{\frac{\partial E_1}{\partial \mathbf{p}} E_2 + E_1 \frac{\partial E_2}{\partial \mathbf{p}}}{E_1^2 E_2^2} (\dot{E}_1 E_2 + E_1 \dot{E}_2) \right] \right. \\
& \quad \cdot \left[\frac{1}{4c^2} \left(\frac{c_\triangleright}{m_1} + \frac{c_\triangleleft}{m_2} \right) + \frac{c_1(E_1 + E_2)}{E_1 E_2} \left(\frac{c_1}{2} \left(\frac{1}{(E_1 + E_2)^2} - \frac{1}{E_1 E_2} \right) - \frac{4}{c^2} \left(\frac{E_1 E_2}{c^2} + p^2 \right) \right) \right] \\
& \quad - \frac{\frac{\partial E_1}{\partial \mathbf{p}} E_2 + E_1 \frac{\partial E_2}{\partial \mathbf{p}}}{E_1 E_2} \left[\frac{\dot{c}_\triangleright}{4c^2} \left(\frac{1}{m_1} + \frac{m_2}{m_1^2} \right) + \left(\frac{\dot{c}_1(E_1 + E_2) + c_1(\dot{E}_1 + \dot{E}_2)}{E_1 E_2} - \frac{c_1(E_1 + E_2)(\dot{E}_1 E_2 + E_1 \dot{E}_2)}{E_1^2 E_2^2} \right) \right. \\
& \quad \cdot \left(\frac{c_1}{2} \left(\frac{1}{(E_1 + E_2)^2} - \frac{1}{E_1 E_2} \right) - \frac{4}{c^2} \left(\frac{E_1 E_2}{c^2} + p^2 \right) \right) \\
& \quad + \frac{c_1(E_1 + E_2)}{E_1 E_2} \left(\frac{\dot{c}_1}{2} \left(\frac{1}{(E_1 + E_2)^2} - \frac{1}{E_1 E_2} \right) + \frac{c_1}{2} \left(-2 \frac{\dot{E}_1 + \dot{E}_2}{(E_1 + E_2)^3} + \frac{\dot{E}_1 E_2 + E_1 \dot{E}_2}{E_1^2 E_2^2} \right) \right. \\
& \quad \left. \left. - \frac{4}{c^2} \left(\frac{\dot{E}_1 E_2 + E_1 \dot{E}_2}{c^2} + 2\mathbf{p} \cdot \dot{\mathbf{p}} \right) \right) \right] \\
& + \frac{1}{4c^2} \left(\frac{1}{m_1} + \frac{m_2}{m_1^2} \right) \frac{d}{dt} \frac{\partial c_\triangleright}{\partial \mathbf{p}} \\
& + \left[\left(\frac{\dot{E}_1 + \dot{E}_2}{E_1 E_2} - \frac{(E_1 + E_2)(\dot{E}_1 E_2 + E_1 \dot{E}_2)}{E_1^2 E_2^2} \right) \frac{\partial c_1}{\partial \mathbf{p}} + \frac{E_1 + E_2}{E_1 E_2} \frac{d}{dt} \frac{\partial c_1}{\partial \mathbf{p}} \right. \\
& \quad + \left(\frac{\dot{c}_1}{E_1 E_2} - \frac{c_1(\dot{E}_1 E_2 + E_1 \dot{E}_2)}{E_1^2 E_2^2} \right) \left(\frac{\partial E_1}{\partial \mathbf{p}} + \frac{\partial E_1}{\partial \mathbf{p}} - \frac{E_1 + E_2}{E_1 E_2} \left(\frac{\partial E_1}{\partial \mathbf{p}} E_2 + E_1 \frac{\partial E_2}{\partial \mathbf{p}} \right) \right) \\
& \quad + \frac{c_1}{E_1 E_2} \left(\frac{d}{dt} \frac{\partial E_1}{\partial \mathbf{p}} + \frac{d}{dt} \frac{\partial E_2}{\partial \mathbf{p}} - \left(\frac{\dot{E}_1 + \dot{E}_2}{E_1 E_2} - \frac{(E_1 + E_2)(\dot{E}_1 E_2 + E_1 \dot{E}_2)}{E_1^2 E_2^2} \right) \left(\frac{\partial E_1}{\partial \mathbf{p}} E_2 + E_1 \frac{\partial E_2}{\partial \mathbf{p}} \right) \right. \\
& \quad \left. - \frac{E_1 + E_2}{E_1 E_2} \left(\frac{d}{dt} \frac{\partial E_1}{\partial \mathbf{p}} E_2 + \frac{\partial E_1}{\partial \mathbf{p}} \dot{E}_2 + E_1 \frac{\partial E_2}{\partial \mathbf{p}} + E_1 \frac{d}{dt} \frac{\partial E_2}{\partial \mathbf{p}} \right) \right) \right] \\
& \quad \cdot \left(\frac{c_1}{2} \left(\frac{1}{(E_1 + E_2)^2} - \frac{1}{E_1 E_2} \right) - \frac{4}{c^2} \left(\frac{E_1 E_2}{c^2} + p^2 \right) \right) \\
& + \left[\frac{E_1 + E_2}{E_1 E_2} \frac{\partial c_1}{\partial \mathbf{p}} + \frac{c_1}{E_1 E_2} \left(\frac{\partial E_1}{\partial \mathbf{p}} + \frac{\partial E_1}{\partial \mathbf{p}} - \frac{E_1 + E_2}{E_1 E_2} \left(\frac{\partial E_1}{\partial \mathbf{p}} E_2 + E_1 \frac{\partial E_2}{\partial \mathbf{p}} \right) \right) \right] \\
& \quad \cdot \left(\frac{\dot{c}_1}{2} \left(\frac{1}{(E_1 + E_2)^2} - \frac{1}{E_1 E_2} \right) + \frac{c_1}{2} \left(-2 \frac{\dot{E}_1 + \dot{E}_2}{(E_1 + E_2)^3} + \frac{\dot{E}_1 E_2 + E_1 \dot{E}_2}{E_1^2 E_2^2} \right) - \frac{4}{c^2} \left(\frac{\dot{E}_1 E_2 + E_1 \dot{E}_2}{c^2} + 2\mathbf{p} \cdot \dot{\mathbf{p}} \right) \right) \\
& + \left(\frac{\dot{c}_1(E_1 + E_2) + c_1(\dot{E}_1 + \dot{E}_2)}{E_1 E_2} - \frac{c_1(E_1 + E_2)(\dot{E}_1 E_2 + E_1 \dot{E}_2)}{E_1^2 E_2^2} \right) \\
& \quad \cdot \left[\frac{1}{2} \frac{\partial c_1}{\partial \mathbf{p}} \left(\frac{1}{(E_1 + E_2)^2} - \frac{1}{E_1 E_2} \right) + \frac{c_1}{2} \left(-2 \frac{\frac{\partial E_1}{\partial \mathbf{p}} + \frac{\partial E_2}{\partial \mathbf{p}}}{(E_1 + E_2)^3} + \frac{\frac{\partial E_1}{\partial \mathbf{p}} E_2 + E_1 \frac{\partial E_2}{\partial \mathbf{p}}}{E_1^2 E_2^2} \right) \right. \\
& \quad \left. - \frac{4}{c^2} \left(\frac{1}{c^2} \left(\frac{\partial E_1}{\partial \mathbf{p}} E_2 + E_1 \frac{\partial E_2}{\partial \mathbf{p}} \right) + 2\mathbf{p} \right) \right]
\end{aligned}$$

$$\begin{aligned}
& + \frac{c_1(E_1 + E_2)}{E_1 E_2} \left[\frac{1}{2} \frac{d}{dt} \frac{\partial c_1}{\partial \mathbf{p}} \left(\frac{1}{(E_1 + E_2)^2} - \frac{1}{E_1 E_2} \right) + \frac{1}{2} \frac{\partial c_1}{\partial \mathbf{p}} \left(-2 \frac{\dot{E}_1 + \dot{E}_2}{(E_1 + E_2)^3} + \frac{\dot{E}_1 E_2 + E_1 \dot{E}_2}{E_1^2 E_2^2} \right) \right. \\
& \quad + \frac{\dot{c}_1}{2} \left(-2 \frac{\frac{\partial E_1}{\partial \mathbf{p}} + \frac{\partial E_2}{\partial \mathbf{p}}}{(E_1 + E_2)^3} + \frac{\frac{\partial E_1}{\partial \mathbf{p}} E_2 + E_1 \frac{\partial E_2}{\partial \mathbf{p}}}{E_1^2 E_2^2} \right) \\
& \quad + \frac{c_1}{2} \left(-\frac{2}{(E_1 + E_2)^3} \left(\frac{d}{dt} \frac{\partial E_1}{\partial \mathbf{p}} + \frac{d}{dt} \frac{\partial E_2}{\partial \mathbf{p}} + \left(\frac{\partial E_1}{\partial \mathbf{p}} E_2 + E_1 \frac{\partial E_2}{\partial \mathbf{p}} \right) (\dot{E}_1 E_2 + E_1 \dot{E}_2) \right) \right. \\
& \quad \left. \left. + 6 \frac{\frac{\partial E_1}{\partial \mathbf{p}} + \frac{\partial E_2}{\partial \mathbf{p}}}{(E_1 + E_2)^3} (\dot{E}_1 + \dot{E}_2) + \frac{1}{E_1^2 E_2^2} \left(\frac{d}{dt} \frac{\partial E_1}{\partial \mathbf{p}} E_2 + \frac{\partial E_1}{\partial \mathbf{p}} \dot{E}_2 + \dot{E}_1 \frac{\partial E_2}{\partial \mathbf{p}} + E_1 \frac{d}{dt} \frac{\partial E_2}{\partial \mathbf{p}} \right) \right) \right] \} \\
& \quad - \frac{4}{c^2} \left(\left(\frac{1}{c^2} \left(\frac{d}{dt} \frac{\partial E_1}{\partial \mathbf{p}} E_2 + \frac{\partial E_1}{\partial \mathbf{p}} \dot{E}_2 + \dot{E}_1 \frac{\partial E_2}{\partial \mathbf{p}} + E_1 \frac{d}{dt} \frac{\partial E_2}{\partial \mathbf{p}} \right) + 2 \dot{\mathbf{p}} \right) \right) \} \\
& \quad (90)
\end{aligned}$$